

STAY-GREEN and Chlorophyll Catabolic Enzymes Interact at Light-Harvesting Complex II for Chlorophyll Detoxification during Leaf Senescence in *Arabidopsis*

Yasuhito Sakuraba,^{a,1} Silvia Schelbert,^{b,1} So-Yon Park,^{a,1,2} Su-Hyun Han,^a Byoung-Doo Lee,^a Céline Besagni Andrés,^c Felix Kessler,^c Stefan Hörtensteiner,^{b,1} and Nam-Chon Paek^{a,1,3}

^a Department of Plant Science, Plant Genomics and Breeding Institute, and Research Institute for Agriculture and Life Sciences, Seoul National University, Seoul 151-921, Korea

^b Institute of Plant Biology, University of Zurich, CH-8008 Zurich, Switzerland

^c Institute of Botany, University of Neuchâtel, CH-2007 Neuchâtel, Switzerland

During leaf senescence, plants degrade chlorophyll to colorless linear tetrapyrroles that are stored in the vacuole of senescing cells. The early steps of chlorophyll breakdown occur in plastids. To date, five chlorophyll catabolic enzymes (CCEs), NONYELLOW COLORING1 (NYC1), NYC1-LIKE, pheophytinase, pheophorbide *a* oxygenase (PAO), and red chlorophyll catabolite reductase, have been identified; these enzymes catalyze the stepwise degradation of chlorophyll to a fluorescent intermediate, *p*FCC, which is then exported from the plastid. In addition, *STAY-GREEN* (SGR), Mendel's green cotyledon gene encoding a chloroplast protein, is required for the initiation of chlorophyll breakdown in plastids. Senescence-induced SGR binds to light-harvesting complex II (LHCII), but its exact role remains elusive. Here, we show that all five CCEs also specifically interact with LHCII. In addition, SGR and CCEs interact directly or indirectly with each other at LHCII, and SGR is essential for recruiting CCEs in senescing chloroplasts. PAO, which had been attributed to the inner envelope, is found to localize in the thylakoid membrane. These data indicate a predominant role for the SGR-CCE-LHCII protein interaction in the breakdown of LHCII-located chlorophyll, likely to allow metabolic channeling of phototoxic chlorophyll breakdown intermediates upstream of nontoxic *p*FCC.

INTRODUCTION

Leaf senescence is a genetically determined and highly ordered process that constitutes the final stage of leaf development. It remobilizes nutrients, in particular nitrogen and phosphorus, to sink organs, such as storage tissues or seeds. On the cellular level, the most significant early changes occur in the chloroplasts, where grana membranes are unstacked and overall thylakoid membrane density is reduced. This catabolic process is accompanied by the massive degradation of chloroplast proteins, which constitute ~70% of total cellular protein (Hörtensteiner and Feller, 2002). By contrast, the chloroplast envelope remains intact late into senescence, indicating that cellular compartmentalization is maintained during senescence (Matile et al., 1999; Thomas et al., 2003). This is in agreement with the observation that leaf senescence can be

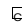
experimentally reversed (Zavaleta-Mancera et al., 1999a, 1999b), up to a "point of no return," beyond which senescence is followed by death (Guiboileau et al., 2010). Hence, cellular senescence is seen as a transdifferentiation rather than a cell death process, and viability needs to be maintained to allow senescence initiation and progression (Thomas et al., 2003).

Loss of green color is the visible symptom of leaf senescence and is caused by the degradation of chlorophyll. In recent years, a pathway has been elucidated that is active during senescence and converts chlorophyll to colorless linear tetrapyrroles, so-called nonfluorescent chlorophyll catabolites (NCCs), as end products of chlorophyll breakdown (Hörtensteiner, 2006; Kräutler, 2008; Hörtensteiner and Kräutler, 2011). The early, plastid-localized reactions of the pathway end with the formation of a primary fluorescent chlorophyll catabolite (*p*FCC). After export from the plastid, several peripheral side chains of *p*FCC are modified in the cytosol to produce a species-specific variety of FCCs. Finally, after import into the vacuole, these modified FCCs are isomerized to their respective NCCs in a nonenzymatic reaction driven by the acidic vacuolar pH (Oberhuber et al., 2003). Interestingly, all except one of the NCCs identified to date are derived from chlorophyll *a*, and conversion from chlorophyll *b* to chlorophyll *a* was shown to be a prerequisite for chlorophyll breakdown (Hörtensteiner et al., 1995; Hörtensteiner and Kräutler, 2011). Consequently, mutants deficient in chlorophyll *b* reductase, catalyzing the first of two consecutive reactions of chlorophyll *b* to chlorophyll *a* reduction, develop a stay-green phenotype and

¹ These authors contributed equally to this work.

² Current address: Division of Plant Sciences, University of Missouri, Columbia, MO 65211.

³ Address correspondence to ncpaek@snu.ac.kr. The authors responsible for distribution of materials integral to the findings presented in this article in accordance with the policy described in the Instructions for Authors (www.plantcell.org) are: Stefan Hörtensteiner (shorten@botinst.uzh.ch) and Nam-Chon Paek (ncpaek@snu.ac.kr).

 Some figures in this article are displayed in color online but in black and white in the print edition.

 Online version contains Web-only data.

retain large quantities of chlorophyll, in particular chlorophyll *b*. In *Arabidopsis thaliana* and rice (*Oryza sativa*), chlorophyll *b* reductase is encoded by two orthologous genes each, *NONYELLOW COLORING1 (NYC1)* and *NYC1-LIKE (NOL)* (Kusaba et al., 2007; Horie et al., 2009; Sato et al., 2009). Recently, 7-hydroxymethyl chlorophyll *a* reductase (HMCR), catalyzing the second step of conversion of chlorophyll *b* to chlorophyll *a*, has been identified at the molecular level (Meguro et al., 2011).

The plastid-located part of the chlorophyll degradation pathway starts with the removal of the central Mg atom by a metal chelating substance, whose molecular nature is as yet unknown, and is followed by phytol hydrolysis yielding pheophorbide (Pheide) *a*. Dephytylation was for a long time considered to be catalyzed by chlorophyllase (i.e., to precede Mg dechelation and to yield chlorophyllide as an intermediate) (Takamiya et al., 2000). However, recent investigation of leaf senescence in *Arabidopsis* and rice showed that, instead, pheophytinase (PPH) is active, which specifically dephytylates pheophytin (Mg-free chlorophyll), but does not accept chlorophyll as substrate (Morita et al., 2009; Schelbert et al., 2009; Ren et al., 2010). Next, the chlorin macrocycle of Pheide *a* is oxygenolytically opened by a Rieske-type monooxygenase, termed Pheide *a* oxygenase (PAO) (Pružinská et al., 2003, 2005). The product of this reaction, red chlorophyll catabolite (RCC), is then reduced to *p*FCC in a regio- and stereo-selective manner catalyzed by RCC reductase (RCCR) (Pružinská et al., 2007). Biochemical and two-hybrid experiments indicated interaction between PAO and RCCR as well as metabolic channeling of RCC (Rodoni et al., 1997; Pružinská et al., 2007). PAO activity provides the structural basis for all further breakdown products (i.e., RCCs, FCCs, and NCCs). Therefore, this pathway is termed the PAO pathway (Hörtensteiner and Kräutler, 2011).

Screening for stay-green mutants in many species uncovered a novel chloroplast-located protein, termed STAY-GREEN (SGR) (Hörtensteiner, 2009), whose function is considered to be related to chlorophyll breakdown, but is not a chlorophyll catabolic enzyme (CCE) itself. SGR was shown to specifically interact with light-harvesting complex subunits of photosystem II (LHCII) but not with core complexes or LHCI subunits (Park et al., 2007). It is assumed that SGR interaction with LHCII may trigger destabilization of these chlorophyll-apoprotein complexes as a prerequisite for the subsequent degradation of both chlorophyll and apoproteins (Park et al., 2007; Hörtensteiner, 2009). In line with this is the observation that besides retention of chlorophyll, *sgr* mutants in various plants also retain large quantities of LHCII subunits (Jiang et al., 2007; Park et al., 2007; Aubry et al., 2008). The same is true for other *sgr* mutants caused by a deficiency in either NYC1 or PPH (Kusaba et al., 2007; Horie et al., 2009; Morita et al., 2009; Schelbert et al., 2009), and it has been assumed that the concerted activity of these three proteins is required for the initiation of LHCII protein degradation during leaf senescence (Schelbert et al., 2009). By contrast, deficiency in PAO or RCCR results in an accelerated cell death phenotype, which is caused by the accumulation of the substrates of respective reactions, Pheide *a* or RCC (Mach et al., 2001; Pružinská et al., 2003, 2005, 2007). These colored intermediates of chlorophyll breakdown are potentially phototoxic, and tight control of the PAO pathway has been considered important to prevent premature cell death during senescence (Hörtensteiner, 2004, 2006).

Using different complementary methods, including yeast two-hybrid analysis, *in vitro* and *in vivo* pull-down assays, and bimolecular fluorescence complementation (BiFC), we provide evidence that SGR and five CCEs, involved in the conversion of chlorophyll to *p*FCC, localize to LHCII and molecularly interact with each other. Hence, during active chlorophyll breakdown, dynamic SGR-CCE-LHCII protein interaction occurs at the thylakoid membrane. The likely role of these interactions is to metabolically channel chlorophyll breakdown pigments to minimize the risk of photodynamism of these light-excitable intermediates and, thus, to prevent accelerated cell death during leaf senescence.

RESULTS

Arabidopsis Plants Expressing Epitope-Tagged SGR or CCEs Exhibit Enhanced Chlorophyll Breakdown during Senescence

During leaf senescence, SGR and five CCEs (RCCR, PAO, PPH, NYC1, and NOL) have been identified as essential components of chlorophyll degradation (Hörtensteiner and Kräutler, 2011).

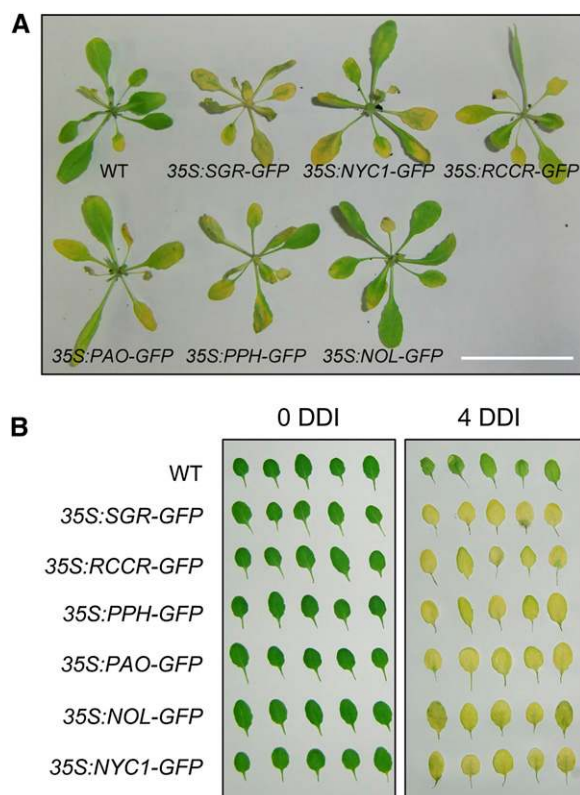


Figure 1. Accelerated Leaf Yellowing of *Arabidopsis* Plants Constitutively Expressing GFP-Tagged SGR or CCEs during Dark-Induced Senescence.

Three-week-old plants grown under long-day conditions were used in this study. Photographs were taken from whole plants (**A**) or detached leaves (**B**) before (0 DDI; **B**) or after incubation in darkness for 4 d (4 DDI; **A**) and (**B**). WT, wild type. Bar = 5 cm.

For this study, we produced *Arabidopsis* transgenic lines that constitutively expressed SGR or one of the five CCEs as fusion proteins with green fluorescent protein (GFP), tandem affinity purification (TAP), or glutathione S-transferase (GST) tags (see Supplemental Table 1 online). Transgenic lines with the highest levels of transgene expression were selected, and correct sizes of fusion proteins were verified by immunoblot analysis using antibodies against GFP (α -GFP), myc (α -myc; for TAP detection), and GST (α -GST). All the GFP-tagged SGR and CCEs were mostly detected in membrane-enriched fractions and barely in soluble fractions of total protein extracts (see Supplemental Figure 1 online).

To examine the effects of constitutive expression of GFP-tagged CCEs on chlorophyll degradation during leaf senescence, we used 3-week-old plants to dark-induce senescence in either whole plants (Figure 1A) or detached leaves (Figure 1B). Before dark incubation (0 d of dark incubation [DDI]), chlorophyll levels and chlorophyll *a/b* ratios (Table 1) of these transgenic plants were almost indistinguishable from the wild-type plants. However, accelerated leaf yellowing (Figure 1) and reduced levels of chlorophyll (Table 1) were observed at 4 DDI in both whole plants and detached leaves compared with the wild-type plants. In addition, because of an assumingly enhanced chlorophyll *b* reductase activity, *35S:NYC1-GFP* and *35S:NOL-GFP* plants exhibited higher chlorophyll *a/b* ratios (Table 1). These plants exhibited a similar phenotype under natural senescence conditions (see Supplemental Figure 2 online). Furthermore, using the *35S:PPH-GFP* line, we analyzed mRNA levels of SGR and the other chlorophyll catabolic genes in green and senescence-induced leaves (see Supplemental Figure 3 online). After senescence induction, SGR, RCCR, PAO, and NYC1, but not NOL, were significantly higher expressed in the *PPH-GFP* over-expressing plants than in the wild-type plants. These results indicate that constitutive expression of GFP-tagged CCEs is not

sufficient to activate chlorophyll degradation during vegetative growth, but significantly accelerates chlorophyll degradation during leaf senescence, likely through transcriptional coactivation of other genes of the pathway.

SGR and CCEs Specifically Interact with LHCII at the Thylakoid Membrane

Previously, we showed that SGR interacts with LHCII *in vitro* and *in vivo* (Park et al., 2007). Using α -GFP-conjugated beads for *in vivo* pull-down assays with membrane-enriched fractions of non-senescent (0 DDI) or senescence-induced (3 DDI) *35S:SGR-GFP* plants, we found that SGR-GFP, which is constitutively present in this line, interacts with LHCII regardless of the senescence conditions (see Supplemental Figure 4 online). We extended this analysis by testing whether CCEs also interact with LHCII and/or other photosystem proteins. For this, we performed *in vivo* pull-down assays with non-senescent (0 DDI) GFP- or GST-tagged transgenic plants using α -GFP- and α -GST-conjugated beads, respectively, followed by immunoblot analysis with antibodies against three photosystem proteins (α -Lhcb1, α -Lhca1, and α -CP43). Like SGR (Figure 2A), all five CCE proteins were coimmunoprecipitated with Lhcb1, but not with Lhca1 or CP43 (Figures 2B to 2F), indicating that not only SGR but also chloroplast-located CCEs bind to LHCII at the thylakoid membrane.

Simultaneous Pull-Down of SGR and CCEs at the Thylakoid Membrane in Senescing Chloroplasts

The interaction of SGR and the five CCEs with LHCII indicated the formation of a large chlorophyll catabolic complex for chlorophyll breakdown during leaf senescence. To investigate this possibility, *35S:PPH-GFP* plants were employed for *in vivo* pull-down assays. To this end, intact plants were senescence-induced by 3 DDI,

Table 1. Chlorophyll Levels of 3-Week-Old Transgenic *Arabidopsis* Plants Expressing Tagged Versions of SGR and CCEs

<i>Arabidopsis</i>		Before Dark Incubation (0 DDI)				After 4 DDI				
		Total Chlorophyll ^a		Chlorophyll <i>a/b</i> Ratio		Total Chlorophyll ^a		Chlorophyll <i>a/b</i> Ratio		
Transformants	Sample No.	Mean	SD	Mean	SD	Sample No.	Mean	SD	Mean	SD
Whole plants										
Wild type	7	1885	43	3.23	0.09	7	1323	83	3.27	0.23
<i>35S:SGR-GFP</i>	6	1821	32	3.17	0.23	7	213	45	2.88	0.29
<i>35S:RCCR-GFP</i>	5	1877	33	3.32	0.19	7	477	54	3.02	0.33
<i>35S:NYC1-GFP</i>	6	1865	54	3.39	0.16	7	305	52	4.41	0.40
<i>35S:NOL-GFP</i>	5	1760	31	3.72	0.25	6	899	102	4.65	0.31
<i>35S:PPH-GFP</i>	7	1843	43	3.28	0.18	8	534	65	3.54	0.16
<i>35S:PAO-GFP</i>	5	1885	48	3.29	0.18	7	455	79	3.32	0.29
Detached leaves										
Wild type	5	1865	25	3.21	0.07	7	1026	64	3.12	0.21
<i>35S:SGR-GFP</i>	7	1818	53	3.32	0.17	7	86	21	3.02	0.20
<i>35S:RCCR-GFP</i>	7	1892	61	3.52	0.18	7	213	43	2.88	0.29
<i>35S:NYC1-GFP</i>	7	1954	23	3.42	0.14	7	132	34	4.62	0.23
<i>35S:NOL-GFP</i>	6	1734	49	3.89	0.19	6	343	69	4.98	0.42
<i>35S:PPH-GFP</i>	5	1865	13	3.34	0.21	8	214	55	3.54	0.19
<i>35S:PAO-GFP</i>	7	1834	24	3.23	0.11	7	177	42	3.98	0.28

^aUnit of total chlorophyll is nmol mg⁻¹ fresh weight.

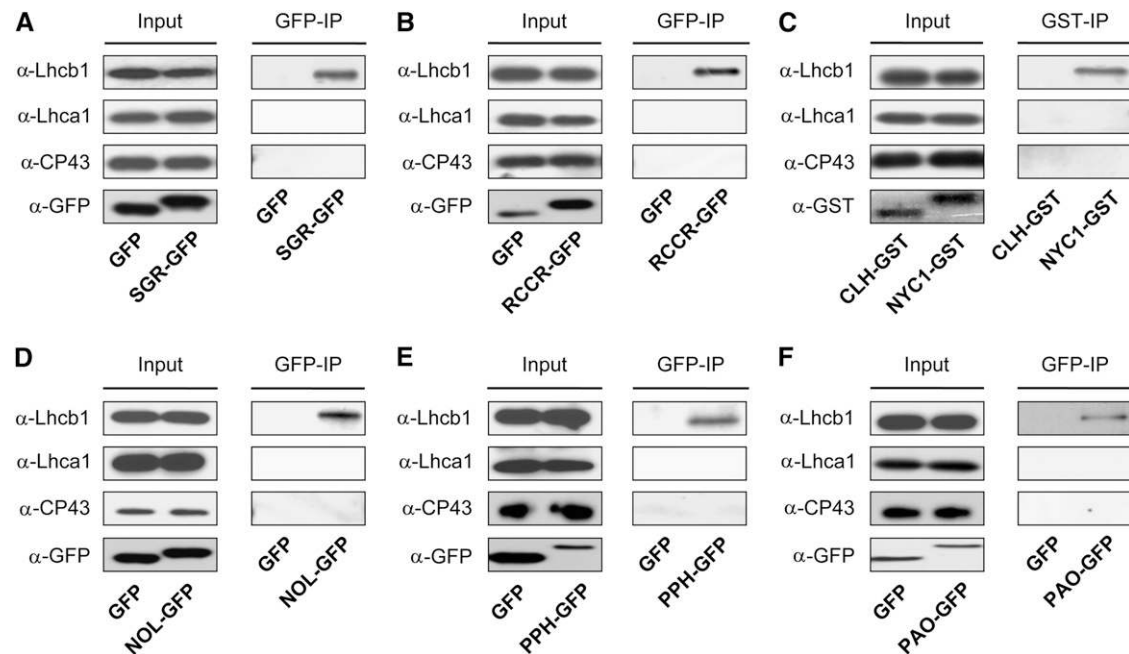


Figure 2. CCEs Interact with LHCII in Vivo.

In vivo interactions of tagged SGR (A), RCCR (B), NYC1 (C), NOL (D), PPH (E), or PAO (F) with photosystem proteins were examined with α -Lhcb1, α -Lhca1, and α -CP43. Membrane-enriched fractions of 3-week-old GFP- or GST-tagged plants at 0 DDI were used for pull-down experiments with α -GFP- (GFP-IP) or α -GST-conjugated beads (GST-IP). Total protein extracts from nonsenescent rosette leaves of *35S:SGR-GFP* plants were used as a positive control (Park et al., 2007), and *35S:GFP* and *35S:CLH-GST* plants were used as negative controls. Input levels of tagged proteins and of Lhcb1, Lhca1, and CP43 (all detected with respective antibodies) are shown as loading controls. Note that CLH, whose participation in chlorophyll breakdown has been questioned recently (Schenk et al., 2007), was unable to pull down LHCII (C).

and the membrane-enriched fractions were treated with α -GFP-conjugated beads. As revealed using α -SGR, α -RCCR, α -PAO, α -NYC1, and α -NOL, we found that all tested endogenous proteins (i.e., SGR, RCCR, PAO, NYC1, and NOL) were coimmunoprecipitated with PPH-GFP (Figure 3).

Pairwise Interactions among SGR and CCEs in Yeast Two-Hybrid and in Vitro Pull-Down Assays

Although the results shown in Figure 3 supported the possibility of multiprotein complex formation, they left the question open, whether the observed coimmunoprecipitation between SGR and CCEs solely occurred through their interaction with LHCII or through sole bilateral interaction between pulled PPH and the other proteins, or whether more complex patterns of direct interaction might exist among SGR and CCEs. For example, in vitro interactions of NYC1-NOL and PAO-RCCR have been reported (Pružinská et al., 2007; Morita et al., 2009). To address this, we first examined pairwise interactions among them by measuring β -galactosidase activity in yeast two-hybrid assays (see Methods for further details). We found significant interactions between SGR and each of the five CCEs and between RCCR and the other four CCEs (Figure 4). Among the latter CCEs (PAO, PPH, NYC1, and NOL), only interactions of PAO-PPH and NYC1-NOL were significant. To eliminate possible interference of the N-terminal chloroplast-targeting sequences of the proteins investigated in the yeast two-hybrid assays, we further examined

pairwise interactions by in vitro pull-down assays using the membrane-enriched fractions of GFP-tagged transgenic lines (Figure 5; see Supplemental Figure 5 online). The results were consistent with the yeast two-hybrid interactions (Figure 4). Together, these data strongly suggested that SGR (and possibly RCCR) may act as key players to recruit other CCEs into a possible multiprotein complex for rapid and safe chlorophyll breakdown during leaf senescence.

In Vivo Interactions among SGR and CCEs in Senescing Chloroplasts

Next, we used BiFC as an alternative method to analyze pairwise interactions among SGR and CCEs in vivo (Figure 6; see Supplemental Figure 6 online). Different combinations of SGR-CCE proteins that were fused to either the N- or C-terminal half of yellow fluorescent protein (YFPn or YFPc, respectively) were cotransformed into mesophyll protoplasts isolated from 0 DDI green or 4 DDI senescent leaf tissues. As a positive control for protein-protein interaction that is unrelated to chlorophyll breakdown, we used the two halves of YFP fused to either phosphoribulokinase (PRK) or chloroplast protein 12 (CP12), two proteins that have been shown to form a complex in chloroplasts (Scheibe et al., 2002) (Figure 6B). Most positive interactions among SGR and CCEs described above (Figures 4 and 5; see Supplemental Figure 5 online), including SGR-PAO and NYC1-NOL, also gave positive BiFC fluorescence signals (Figure 6A; see Supplemental

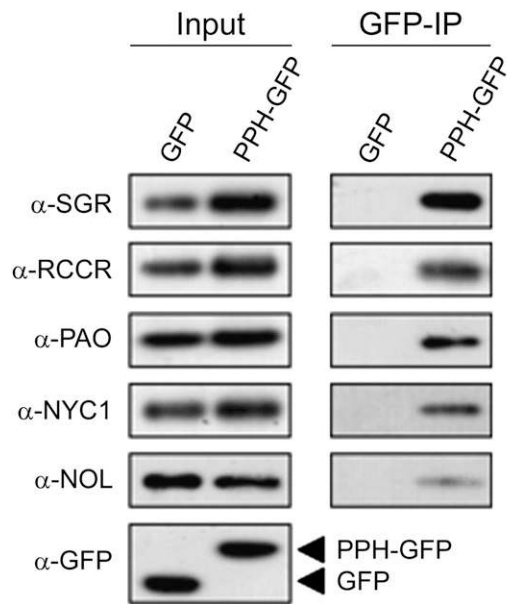


Figure 3. Coimmunoprecipitation of All CCEs and SGR in Senescing Chloroplasts.

35S:GFP and *35S:PPH-GFP* transgenic plants grown for 3 weeks under long-day conditions were transferred to darkness and sampled at 3 DDI. Membrane-enriched fractions were used for *in vivo* pull-down assays. For this, GFP was immunoprecipitated (GFP-IP) with α -GFP-conjugated beads. Native SGR, RCCR, PAO, NYC1, and NOL in the input samples (left panel) and the pulled fractions (right panel) were detected using respective antibodies. The expression of GFP (negative control) and PPH-GFP were confirmed by α -GFP.

Figure 6 online). However, we were unable to verify the *in vitro* interaction of SGR-PPH or SGR-NOL, notably combinations that resulted in rather weak interaction in yeast two-hybrid assays (Figure 4). Surprisingly, YFP fluorescence signals were only obtained in protoplasts isolated from senescent leaves (4 DDI) but not in nonsenescent protoplasts (0 DDI) (Figure 6A).

Based on yeast two-hybrid and *in vitro* pull-down analysis, we suggested that SGR may act as a key player for protein interaction. In order to address this possibility, we analyzed *in vivo* interaction between PAO and RCCR in the *Arabidopsis sgr* mutant, *nye1-1* (Ren et al., 2007), by BiFC. In contrast with the wild type, YFP fluorescence was absent in senescent protoplasts of *nye1-1*. Functionality of the *nye1-1* protoplasts was confirmed by positive YFP fluorescence when using the PRK/CP12 control. These results indicated that presence of SGR in senescing chloroplasts is a prerequisite for CCE protein interaction.

Taking all the results together, we propose that SGR and CCEs interact directly and indirectly with each other to possibly form a large SGR-CCE-LHCII multiprotein complex at the thylakoid membrane during leaf senescence.

PAO Localizes to the Thylakoid Membrane

Based on their primary structures, all CCEs except PAO and NYC1 are soluble proteins. NYC1 and NOL have been shown to

localize at the thylakoid membrane in rice (Sato et al., 2009). By contrast, PAO activity was attributed to the chloroplast envelope in barley (*Hordeum vulgare*; Matile and Schellenberg, 1996), and proteome analyses also favored envelope localization for PAO in *Arabidopsis* (Joyard et al., 2009). However, this proposed envelope localization of PAO conflicted with its proposed interaction with LHCII, SGR, and other CCEs at the thylakoid membrane as described here. Therefore, we readdressed the subchloroplast localization of PAO in mesophyll protoplasts by transiently expressing a PAO-GFP fusion protein (Figure 7). As a positive control for inner envelope localization, we used a GFP-tagged translocon at the inner chloroplast envelope 110 (TIC110-GFP), a component of the chloroplast protein import machinery. PAO-GFP fluorescence signals entirely overlapped with chlorophyll autofluorescence, whereas TIC110-GFP specifically labeled the chloroplast envelope (Figure 7A). In addition, using the wild-type plants, we separated chloroplast membranes by Suc density gradient centrifugation and investigated the distribution of PAO along with chloroplast membrane marker proteins by immunoblot

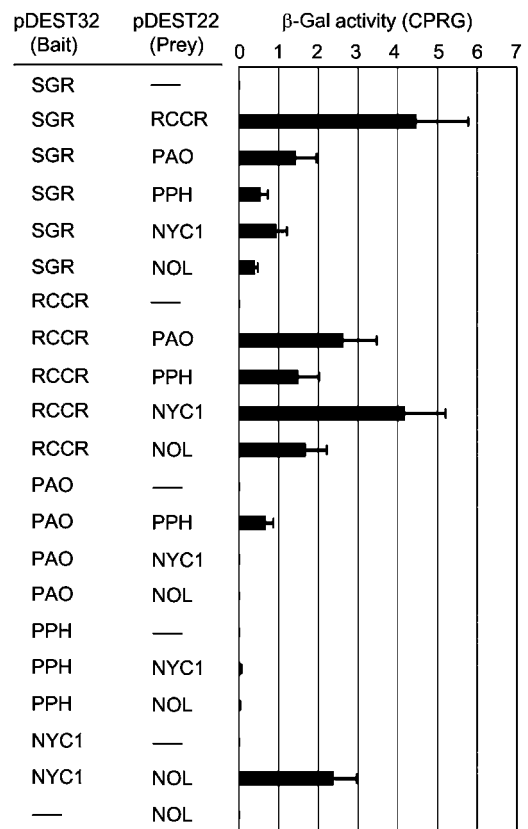


Figure 4. Interactions among SGR and Five CCEs in Yeast Two-Hybrid Assays.

β -Galactosidase (β -Gal) activities in yeast two-hybrid assays were measured by a liquid assay using chlorophenol red- β -D-galactoside (CPRG) as substrate according to the Yeast Protocols Handbook (Clontech). Empty bait or prey plasmids (—) were used as negative controls. Values are the average of relative activity from four colonies, and error bars represent SD.

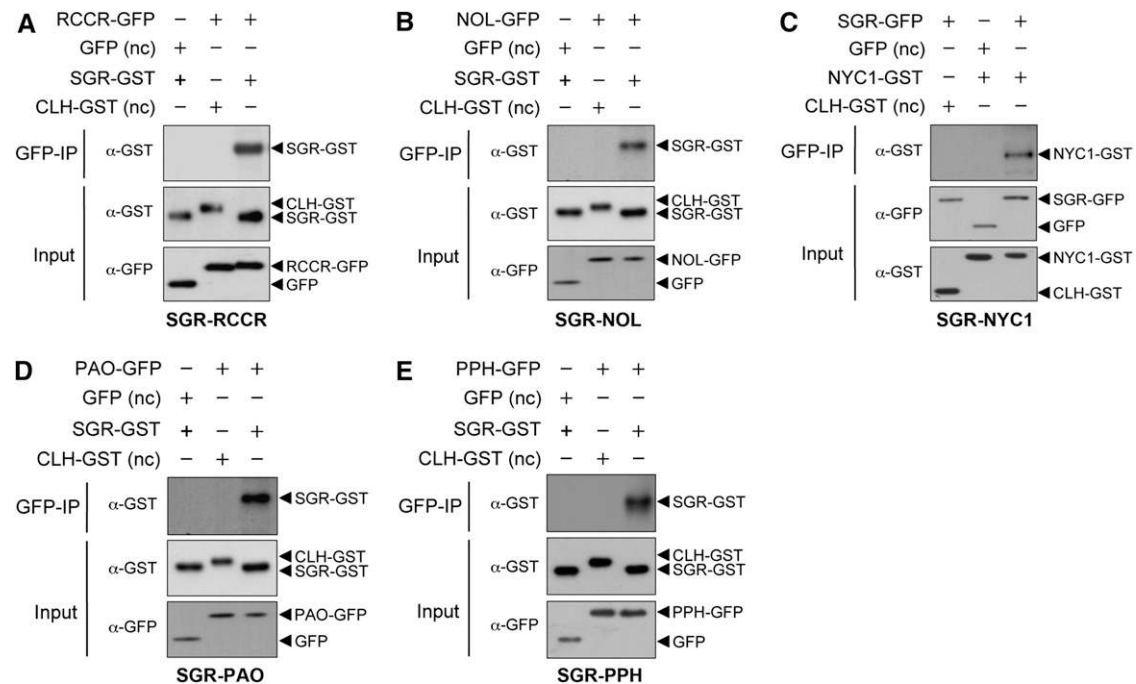


Figure 5. Interactions between SGR and CCEs by in Vitro Pull-Down Assays.

Equal fresh weight of rosette leaves of two 3-week-old *Arabidopsis* plants expressing GFP- or GST-tagged SGR and CCEs were homogenized. Membrane-enriched fractions were used for pull-down assays with α -GFP-conjugated beads (GFP-IP), followed by immunoblot analysis using α -GST. Five combinations, including SGR-RCCR (A), SGR-NOL (B), SGR-NYC1 (C), SGR-PAO (D), and SGR-PPH (E), were examined. *35S::GFP* and *35S::CLH-GST* plants were used as negative controls (nc). Input levels of tagged proteins detected with respective antibodies are shown. Note that none of the GFP-tagged CCEs were able to pull down GST-tagged CLH, indicating that CLH is not part of a chlorophyll breakdown complex. This is in agreement with recent data questioning the involvement of CLH in chlorophyll breakdown (Schenk et al., 2007).

analysis of individual density gradient fractions (Figure 7B). PAO clearly comigrated with chlorophyll *a/b* binding proteins (CAB) but not with an envelope (TOC75) or a plastoglobule (PGL35) marker. Together, these data indicate a thylakoid rather than an envelope localization of PAO, which is in agreement with the finding presented here that PAO is a component of a possible chlorophyll degrading protein complex at the thylakoid membrane.

DISCUSSION

Chlorophyll breakdown is an integral process of senescence, the final part of leaf development. In this respect, loss of green color visually marks the initiation of dramatic metabolic changes that occur during this final phase of development (Lim et al., 2007). Among other processes, senescence is accompanied by a loss of photosynthetic capacity and the massive degradation of cellular proteins. These processes remobilize nutrients from senescing leaves and occur in living cells (i.e., before the ultimate death of the cell). However, chlorophyll breakdown is seen as a detoxification rather than a remobilization process (Hörtensteiner, 2009; Hörtensteiner and Kräutler, 2011). This view is supported by the fact that NCCs, identified as final products of chlorophyll breakdown (Kräutler et al., 1991; Kräutler, 2008), do not absorb visible light and thus are photodynamically safe; however, they still contain the four moles of nitrogen that are also present in chlorophyll. Furthermore, downstream steps of chlorophyll breakdown

(i.e., FCC hydroxylation, conjugation, and excretion to the vacuole) resemble the three-step process of plants that is active for the detoxification of toxic endogenous and xenobiotic compounds, such as herbicides (Kreuz et al., 1996). Finally, mutants that are defective in several steps of chlorophyll breakdown develop an accelerated cell death phenotype, which has been attributed to the accumulation of respective phototoxic chlorophyll breakdown intermediates (Pružinská et al., 2003, 2005, 2007; Tanaka et al., 2003). Among the chlorophyll breakdown intermediates generated in the PAO pathway, all the ones upstream of *p*FCC have the potential to generate singlet oxygen in light, causing toxicity. All this information implies that the steps of chlorophyll breakdown required to produce *p*FCC need to be tightly controlled and accumulation of chlorophyll intermediates upstream of *p*FCC must be prevented or minimized during senescence.

Here, we show that such a control could, at least in part, be accomplished by metabolic channeling of chlorophyll to *p*FCC through dynamic interaction between SGR and CCEs, thereby likely forming a multiprotein complex, which specifically interacts with LHCII (Figure 8).

Possible Formation of a CCE Complex at the Thylakoid Membrane and Specific Interaction with LHCII

The results of these experiments, which included different in vitro and in vivo methods, are summarized in Supplemental Figure 7

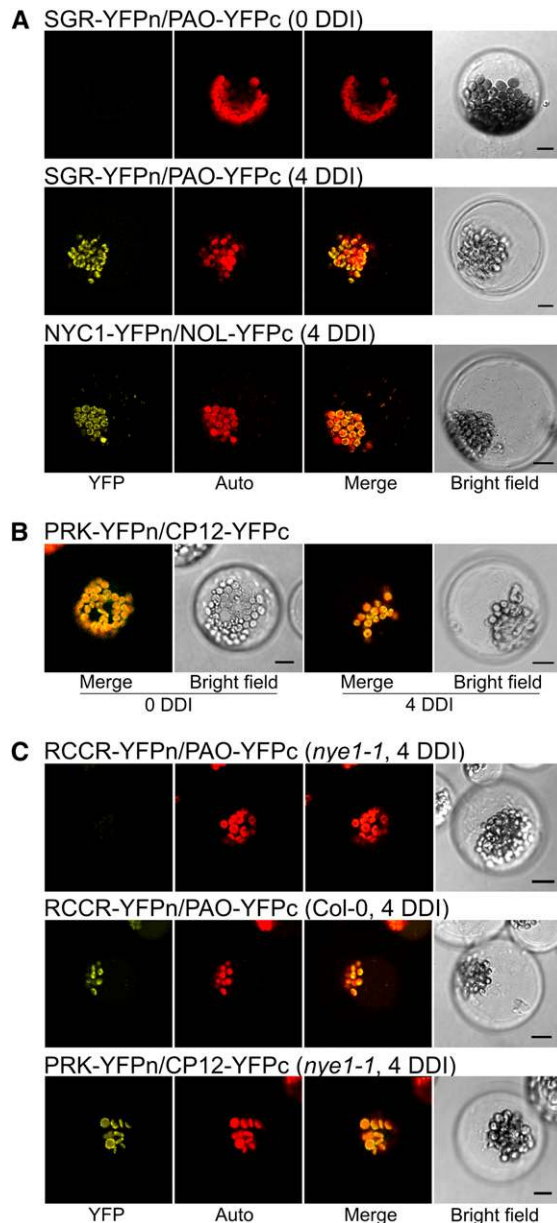


Figure 6. In Vivo Interactions among SGR and CCEs Analyzed by BiFC.

(A) For BiFC assays, construct pairs expressing fusions between SGR, PAO, NYC1, or NOL, and the N- or C-terminal half of YFP (YFPn or YFPc, respectively), were coexpressed in *Arabidopsis* mesophyll protoplasts isolated from 0 DDI green or 4 DDI senescing leaves. Confocal microscopy analysis was performed after 24 h. Note that YFP fluorescence was not detected at 0 DDI. Further positive BiFC interactions among SGR and CCEs are shown in Supplemental Figure 6 online. Auto, chlorophyll autofluorescence. Bars = 10 μ m.

(B) As a positive control for chloroplast-located BiFC interaction, PRK and CP12 fusions were used. Note that positive interaction was detected in both 0 DDI and 4 DDI protoplasts. Bars = 10 μ m.

(C) BiFC interaction between PAO and RCCR was positive in the wild-type protoplasts at 4 DDI but negative in the *Arabidopsis sgr* mutant *nye1-1*. As a control, positive interaction of PRK and CP12 was demonstrated in *nye1-1*. Bars = 10 μ m.

online. Not all tested pairwise protein combinations resulted in positive interaction, and different methods yielded partially different results. It remains unclear, however, whether this was due to limitations of the used respective methods or whether this might indicate rather dynamic and possibly only transient interaction among SGR and CCEs in vivo. Nevertheless, in vivo pull-down experiments (Figure 3) confirmed coimmunoprecipitation of all tested CCEs and SGR, indicating that they indeed might form a multiprotein complex, possibly with varying protein composition.

We considered the thylakoid membrane as the likely site of protein interaction because SGR had been demonstrated to interact with LHCII (Park et al., 2007), and NYC1, in complex with NOL, had been suggested to localize to thylakoids (Sato et al., 2009). Here, we provide evidence that also PAO, which had been proposed to localize to the chloroplast envelope (Matile and Schellenberg, 1996; Joyard et al., 2009), resides in thylakoid membranes (Figure 7). Using in vivo pull-down experiments, we demonstrate that the SGR/CCE complex components specifically interact with LHCII (Figure 2), in agreement with the presence of GFP-tagged SGR/CCE proteins in membrane-enriched fractions rather than soluble fractions (see Supplemental Figure 1 online). This specificity for LHCII is surprising because during senescence, chlorophyll in both LHCI and LHCII (and probably also core complexes) is degraded. In accordance with this, *sgr* mutants retain both LHCI and LHCII subunits during senescence (Park et al., 2007; Sato et al., 2007), suggesting the involvement of SGR in chlorophyll degradation in the antenna of both photosystems. Nevertheless, SGR specifically binds to LHCII (Figure 2; see Supplemental Figure 4 online) (Park et al., 2007). By contrast, other *sgr* mutants that are deficient in PPH or NYC1 specifically retain LHCII subunits, with comparably minor alterations of LHCI compared with the wild-type plants (Kusaba et al., 2007; Horie et al., 2009; Morita et al., 2009; Sato et al., 2009; Schelbert et al., 2009). This together with a particularly high retention of chlorophyll *b* in these mutants, which is indicative of a LHCII-related defect, challenges their role in degradation of chlorophyll from LHCI. However, we cannot rule out the possibility that SGR/CCEs might interact with other LHCI subunits, which were not tested in this work. In summary, published data are conflicting with respect to the specificity of SGR/CCEs for particular LHCS, but the data presented here indicate an interaction of SGR/CCEs specifically with LHCII, leaving open the question whether degradation of LHCI-located chlorophyll involves CCEs without direct contact to LHCI or whether other, so far unknown, enzymes or localizing proteins are required.

Regulatory Role of SGR

Among the different experiments that we performed to demonstrate SGR/CCE interactions, BiFC analysis yielded particularly interesting results because, despite the use of a constitutive 35S promoter for expression, none of the positive interactions observed in senescent protoplasts were found in the wild-type protoplasts before senescence induction (Figure 6). By contrast, interactions of SGR/CCEs with LHCII were senescence independent when constitutively expressing particular

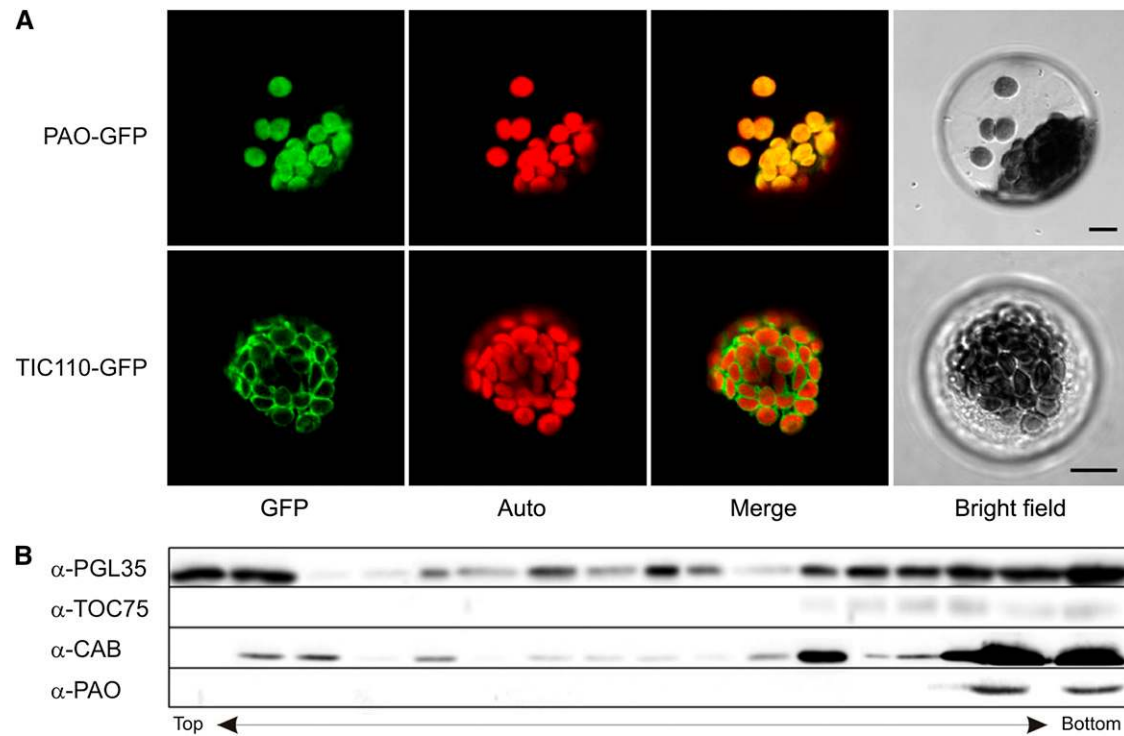


Figure 7. PAO Localizes to the Thylakoid Membrane.

(A) Transient expression of PAO-GFP in the *Arabidopsis* mesophyll protoplasts. Note that GFP fluorescence largely superimposed chlorophyll autofluorescence (Auto), while an envelope control, TIC110-GFP, specifically labeled the surrounding of chloroplasts.

(B) Immunoblot analysis of chloroplast membranes isolated from the 2 DDI senescent leaves after Suc density gradient centrifugation. PAO was visualized in gradient fractions using α -PAO, and its migration was compared with marker proteins from thylakoids (CAB), envelope (TOC75), and plastoglobules (PGL35). PAO largely comigrated with CAB, but not with TOC75 or PGL35, indicating thylakoid localization.

SGR/CCE proteins (see Supplemental Figure 4 online). Thus, SGR/CCEs could most likely also bind to LHCII in BiFC experiments at 0 DDI. Despite this, SGR/CCEs interaction was not observed at 0 DDI, implying that additional, senescence-specific components were required to allow pairwise interaction of the chlorophyll catabolic proteins under investigation in each experiment. The nature of such potential factors remains elusive, but SGR was a particularly interesting candidate for interaction regulation because SGR does not exhibit a known catalytic activity in chlorophyll breakdown but could have a structural and/or regulatory function instead (Park et al., 2007; Hörtensteiner, 2009). In addition, modulation of SGR abundance seems to correlate with overall chlorophyll breakdown. Thus, it was shown that during dark-induced senescence of PAO-deficient *pao1* and *acd1* mutants, SGR expression is severely inhibited (Park et al., 2007), probably with the aim to decrease levels of chlorophyll breakdown if the PAO pathway is blocked. We used *nye1-1* to test the role of SGR in CCE protein interaction. Indeed, the well-established interaction between PAO and RCCR (Rodoni et al., 1997; Pružinská et al., 2007) that also gave positive BiFC results in senescent wild-type cells was disabled in senescent *nye1-1* protoplasts (Figure 6). This strongly supported the possibility that SGR enables interactions among CCEs after they are bound to LHCII.

Control of Reactive Chlorophyll Metabolites and Mechanism of Chlorophyll-Apoprotein Complex Degradation

The data presented here provide evidence for senescence-related, possibly dynamic, interaction of SGR and CCEs at the thylakoid membrane, specifically interacting with LHCII, that is required for chlorophyll to *p*FCC conversion. Very likely, such SGR-CCE-LHCII protein interaction allows metabolic channeling of chlorophyll breakdown intermediates, thereby minimizing the risk of chlorophyll intermediate accumulation and potential phototoxicity as seen in the mutants deficient in PAO or RCCR (Tanaka et al., 2003; Pružinská et al., 2005, 2007). In line with this, during normal senescence, none of these phototoxic chlorophyll intermediates accumulates (Pružinská et al., 2005, 2007; Schelbert et al., 2009). Furthermore, induction of chlorophyll breakdown in senescent chloroplasts causes in organello accumulation of *p*FCC but not of an upstream intermediate of the pathway (Matile et al., 1992; Ginsburg et al., 1994). Surprisingly, however, the mutants deficient in SGR, NYC1, or PPH (i.e., upstream of phytol cleavage) do not show cell death phenotypes (Kusaba et al., 2007; Ren et al., 2007; Schelbert et al., 2009), although in these mutants, the potential of photodynamic effects through excitation of nondegraded chlorophyll increases. It has been argued that in these *sgr* mutants, chlorophyll is retained

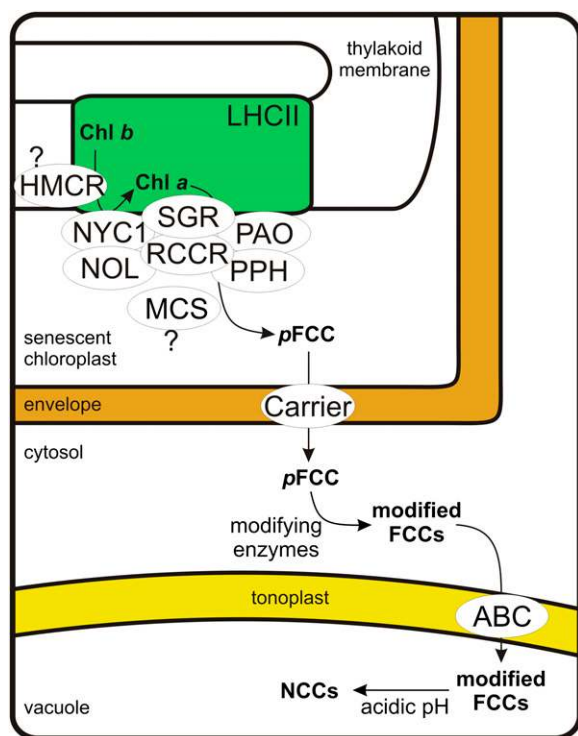


Figure 8. Tentative Model of Chlorophyll Breakdown in a Senescing Mesophyll Cell.

A model depicting the current knowledge about the topology of the PAO pathway, including the results from this work. Breakdown of chlorophyll to *pFCC* tentatively occurs in an enzyme complex located at LHCII in the thylakoid membrane. The exact composition of the complex remains unknown, but the results presented here indicate that SGR and all five CCEs known so far participate. After its formation, *pFCC* is exported from the chloroplast and modified in the cytosol. Modified FCCs are then imported into the vacuole and nonenzymatically converted to respective NCCs. Note that the location and/or participation of HMCR and metal chelating substance (MCS) in the multicomplex is unclear. For simplicity, LHCI and core complex proteins of the photosystems have been omitted. Likewise, the recently discovered hypermodified FCCs formed from *pFCC* in a branched pathway are not shown (Hörtensteiner and Kräutler, 2011). ABC, ABC transporter.

[See online article for color version of this figure.]

within the LHCs. This might shield the photosensitizing properties of chlorophyll, but the mechanism of energy dissipation under these conditions remains to be elucidated (Hörtensteiner and Kräutler, 2011). Likewise, the possible participation of the recently identified HMCR (Meguro et al., 2011) as a further partner for SGR-CCE-LHCII protein interaction remains to be demonstrated.

Chlorophyll breakdown is intimately related to the degradation of chlorophyll binding proteins. While the biochemical pathway of chlorophyll breakdown is largely elucidated, little is known regarding proteases that might be involved in apoprotein degradation (Hörtensteiner and Feller, 2002). Although the kinetics of breakdown of chlorophyll-apoprotein complexes during leaf senescence indicate both components to be degraded in a concerted manner, further open questions remain regarding for example the topological situations. NOL was shown to extract

chlorophyll from LHCII timers *in vitro* (Horie et al., 2009), suggesting that chlorophyll could be released from LHCII even in the presence of the hydrophobic phytol moiety. By contrast, in *sgl* mutants, phytol-harboring chlorophyll is retained within chlorophyll-apoprotein complexes (Park et al., 2007) and degradation of LHCII subunits is limited to a short N-terminal, stroma-facing peptide (Thomas and Howarth, 2000). In view of the results shown here, it could be argued that during senescence, SGR might regulate CCE interaction at chlorophyll-apoprotein complexes to allow immediate capture and degradation of chlorophyll along with the simultaneous proteolytic digestion of the apoproteins.

Do Physical Interaction and Complex Formation Occur during Chlorophyll Biosynthesis?

Metabolome complex formation and metabolic control through channeling likely occurring in chlorophyll breakdown as shown here are known from biosynthetic pathways of several secondary plant compounds (Jørgensen et al., 2005). For chlorophyll biosynthesis, control of metabolite flux is also important. This is seen in the mutants and antisense lines that are impaired in certain steps of chlorophyll synthesis; several of these mutants develop accelerated cell death phenotypes that can be attributed to the accumulation of phototoxic intermediates in chlorophyll synthetic pathway (Tanaka and Tanaka, 2007). However, regulation of chlorophyll intermediate formation during chlorophyll synthesis might be different during chlorophyll degradation. This idea is supported by the fact that besides other regulatory mechanisms, chlorophyll synthesis is under tight metabolic feedback control of δ -amino levulinic acid synthesis, the rate-limiting step of the pathway (Mochizuki et al., 2010), while direct metabolite feedback control has not been demonstrated for a CCE. Furthermore, although pairwise interaction has been demonstrated for some of the chlorophyll synthetic enzymes (Tanaka and Tanaka, 2007), the existence of a hypothetical megacomplex of chlorophyll synthetic enzymes (Shlyk, 1971) remains to be demonstrated (Tanaka and Tanaka, 2007).

METHODS

Plant Materials and Growth Conditions

Arabidopsis thaliana wild-type (Columbia-0 ecotype) and transgenic plants were grown on soil in a growth chamber at 21 to 22°C under cool-white fluorescent light (90 to 100 $\mu\text{mol photons m}^{-2} \text{s}^{-1}$) under long-day (16 h light/8 h dark) conditions. For protoplast transformation and Suc density gradient centrifugation experiments, wild-type plants were grown for 5 and 8 weeks, respectively, at short-day conditions (8 h light/16 h dark) with fluence rates of 100 to 200 $\mu\text{mol photons m}^{-2} \text{s}^{-1}$. Rosette leaves were used for pigment content, immunoblot, and pull-down analyses. For dark-induced senescence of whole plants, 3-week-old plants were transferred to complete darkness. After dark incubation, rosette leaves were sampled under weak green light. For dark treatment of detached leaves, the oldest but still green rosette leaves were incubated on wet filter paper soaked with 3 mM MES, pH 5.7, buffer in complete darkness at 23°C.

Plasmid Construction and *Arabidopsis* Transformation

Arabidopsis full-length cDNAs (no stop codon) of *SGR*, *PPH*, *PAO*, *RCCR*, *NYC1*, and *NOL* were PCR amplified. After insertion into the Gateway

entry vector pCR8/GW/TOPO (Invitrogen), inserts were recombined into the binary Gateway vector pEarleyGate 103, thereby introducing a C-terminal GFP-His tag. In addition, using either pEarleyGate 205 (TAP tag) (Earley et al., 2006) or pCAMBIA-GST (GST tag), we introduced alternative C-terminal tags. The primers used for cloning are listed in Supplemental Table 2 online. In all cases, transgene expression was driven by the constitutive 35S promoter. *Arabidopsis* transgenic plants (see Supplemental Table 1 online) were obtained by *Agrobacterium tumefaciens* (strain GV3101)-mediated transformation through a floral dipping method (Zhang et al., 2006). As negative controls, transgenic plants transformed with empty pEarleyGate 103 or pEarleyGate 205 or with a chlorophyllase 1 (*CLH1*; At1g19670)-GST fusion construct were used. Transgenic plants were selected based on the highest expression of tagged proteins in 2 DDI leaf tissues as determined by immunoblot analysis using α -myc (for TAP detection; Santa Cruz Biotechnology), α -GST (Santa Cruz Biotechnology), or α -GFP (Abcam).

Gene Expression Analysis

The mRNA levels of *SGR* and *CCE* genes were measured by quantitative real-time PCR (qRT-PCR) analysis. Total RNA was extracted from the rosette leaves using the Total RNA Extraction Kit including RNase-free DNase (iNTRON Biotechnology). First-strand cDNA was synthesized with 5 μ g of total RNA using M-MLV reverse transcriptase and an oligo(dT)₁₅ primer (Promega) in 20 μ L mixture. Then, the reaction was diluted fivefold with water and the cDNA used as template for qRT-PCR. The qRT-PCR mixture (20 μ L) contained 2 μ L of cDNA template, 10 μ L of 2 \times LightCycler 480 SYBR Green I Master (Roche), and 0.25 μ M of forward and reverse primers for each gene (see Supplemental Table 2 online). Reactions were performed using the Light Cycler 2.0 instrument (Roche Diagnostics). The transcript levels of each gene were normalized against those of *GAPDH* (glyceraldehyde phosphate dehydrogenase; At1g16300) as previously reported (Sakuraba et al., 2010).

Yeast Two-Hybrid Assay

Arabidopsis full-length cDNAs of *SGR*, *NYC1*, *NOL*, *PPH*, *PAO*, and *RCCR* in entry vectors were inserted into the destination vectors pDEST32 (bait) and pDEST22 (prey) (Invitrogen). The yeast strain MaV203 was used for cotransformation of the bait and prey clones, and β -galactosidase activity assays were performed by a liquid assay using chlorophenol red- β -D-galactoside (Roche Applied Science) according to the Yeast Protocols Handbook (Clontech).

BiFC Analysis

Full-length cDNAs of *SGR* and *CCE* genes were PCR amplified using *Pfu* polymerase (Promega) with the gene-specific primers listed in Supplemental Table 2 online. The PCR products were digested with *Bsp*HI-NotI and cloned via *Nco*I-NotI into pSY728 and pSY738, respectively (Bracha-Drori et al., 2004), thereby producing C-terminal fusions with the N- and C-terminal halves of YFPs (YFPn and YFPc), respectively. After verifying the inserts by sequencing, constructs were used for BiFC studies.

Arabidopsis mesophyll protoplasts were isolated from either green (0 DDI) or senescent leaves at 4 DDI according to published procedures (Endler et al., 2006). Cell numbers were quantified with a Neubauer chamber and adjusted to a density of 2×10^6 protoplasts mL⁻¹. Protoplasts were cotransformed with each two constructs by 20% polyethylene glycol transformation according to published procedures (Meyer et al., 2006). Twenty micrograms of plasmid of each construct was used. Transformed cells were incubated for 24 h in the dark at room temperature before laser scanning confocal microscopy analysis (DM IRE2; Leica Microsystems). YFP fluorescence was imaged at an excitation wavelength of 512 nm, and the emission signal was recovered

between 525 and 565 nm. CP12-YFPc and PRK-YFPn constructs were used as a positive control for plastid colocalization.

PAO-GFP Fusion Protein Analysis

To examine the localization of PAO in chloroplasts, a full-length cDNA of PAO (Pružinská et al., 2003) was PCR amplified using *Pfu* polymerase (Promega) with the primers listed in Supplemental Table 2 online and cloned into *Bam*HI-*Spe*I-restricted pUC18-GFP5T-sp (Meyer et al., 2006), thereby producing a C-terminal fusion with GFP (PAO-GFP). Transient transformation of *Arabidopsis* mesophyll protoplasts and confocal microscopy analysis were performed as described above. GFP fluorescence was imaged at an excitation of 488 nm and emission between 495 and 530 nm. As a control for chloroplast envelope localization, a TIC110-GFP construct was employed (Schelbert et al., 2009).

Pigment Analysis

Chlorophyll was extracted from rosette leaf tissues using ice-cold acetone. Extracts were centrifuged at 15,000 rpm for 10 min at 10°C. The supernatant was diluted with ice-cold water to the final acetone concentration of 80%. Chlorophyll was quantified spectrophotometrically as previously published (Porra et al., 1989).

SDS-PAGE and Immunoblot Analysis

Membrane and soluble proteins were extracted from rosette leaves using the Native Membrane Protein Extraction Kit (Calbiochem). Protein extracts were suspended with an equal volume of 2 \times sample buffer (50 mM Tris, pH 6.8, 2 mM EDTA, 10% [w/v] glycerol, 2% SDS, and 6% 2-mercaptoethanol), denatured at 75°C for 3 min, and subjected to SDS-PAGE. For visualization of protein bands, gels were stained with Coomassie Brilliant Blue (Sigma-Aldrich). The resolved proteins were electroblotted onto Immobilon-P transfer membranes (Millipore). Antibodies against *SGR* (Park et al., 2007), *RCCR* (Pružinská et al., 2007), *PAO* (Pružinská et al., 2005), *NYC1* and *NOL* (Sato et al., 2009), *GFP* (Abcam), *GST* (Santa Cruz Biotechnology), *TOC75* and *PGL35* (Vidi et al., 2006), and photosystem protein antibodies (*CAB* [Vidi et al., 2006], *Lhcb1*, *Lhcb1*, and *CP43*; Agrisera, Sweden) were used for immunoblot analysis. Peroxidase activity of secondary antibodies was visualized using the chemiluminescence detection kit WEST SAVE (AbFRONTIER) or ImmunStar WesternC (Bio-Rad) according to the manufacturers' protocols.

In Vitro and in Vivo Pull-Down Assays

Three-week-old transgenic plants were homogenized with the Native Membrane Protein Extraction Kit (Calbiochem), and membrane-enriched fractions were pulled down using IgG or glutathione agarose beads (Santa Cruz Biotechnology) or α -GFP-conjugated beads (MBL). Precipitated beads were washed at least three times with washing buffer (50 mM Tris-HCl, pH 7.2, 200 mM NaCl, 0.1% Nonidet P-40, 2 mM EDTA, and 10% glycerol). Washed beads were boiled with 20 μ L of 2 \times SDS sample buffer for 5 min and subjected to SDS-PAGE and immunoblot analysis.

Suc Density Gradient Centrifugation

Intact chloroplasts were isolated and the chloroplast membrane fraction was prepared for density gradient centrifugation as described (Vidi et al., 2006). A linear gradient of Suc between 5 and 45% was employed to separate membrane fractions by centrifugation at 100,000g for 17 h (Vidi et al., 2006). One-milliliter fractions were collected starting from the top of the gradient and fractions were analyzed by SDS-PAGE and immunoblot analysis.

Accession Numbers

Sequence data from this article can be found in the Arabidopsis Genome Initiative or GenBank/EMBL databases under the following accession numbers: *SGR/NYE1*, At4g22920; *RCCR*, At4g37000; *NYC1*, At4g13250; *NOL*, At5g04900; *PPH*, At5g13800; *PAO*, At3g44880; *CLH*, At1g19670; and *GAPDH*, At1g16300.

Supplemental Data

The following materials are available in the online version of this article.

Supplemental Figure 1. Subcellular Localization of SGR-GFP and CCE-GFP Fusion Proteins in Transgenic Plants.

Supplemental Figure 2. Natural Senescence of *Arabidopsis* SGR and CCE Overexpressors.

Supplemental Figure 3. Expression Analysis of Genes Encoding SGR and four CCEs in Wild-Type and *35S:PPH-GFP* Leaves by qRT-PCR.

Supplemental Figure 4. *Arabidopsis* SGR Interacts with LHCI in Senescing as well as Nonsenescent Chloroplasts.

Supplemental Figure 5. Interactions among CCEs by in Vitro Pull-Down Assays.

Supplemental Figure 6. In Vivo Interactions among SGR and CCEs Analyzed by BiFC.

Supplemental Figure 7. Possible Metabolic Channeling of Chlorophyll Catabolic Intermediates by Interaction of SGR, CCEs, and LHCI at the Thylakoid Membrane.

Supplemental Table 1. *Arabidopsis* Transformants Expressing a Tagged Version of SGR and CCEs Used in This Study.

Supplemental Table 2. Primers Used in This Study.

ACKNOWLEDGMENTS

We thank John Gray for antibodies against PAO, Ayumi Tanaka for antibodies against NYC1 and NOL, and Benke Kuai for *nye1-1* seeds. This work was supported by grants from the National Research Foundation of Korea funded by the Korean government (2011-0017308 to N.-C.P.) and the Swiss National Science Foundation (to S.H.).

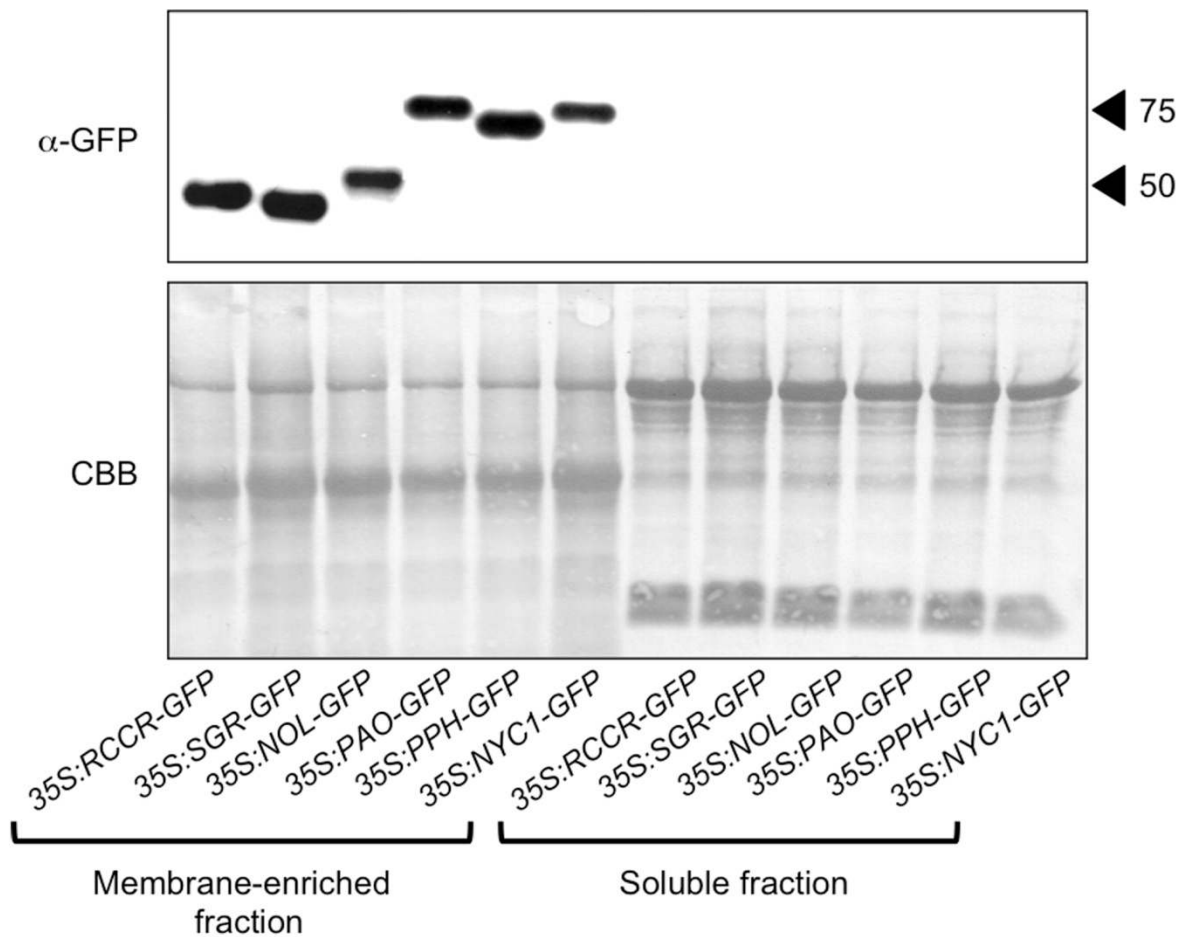
AUTHOR CONTRIBUTIONS

N.-C.P. and S.H. designed research. Y.S., S.S., and S.-Y.P. performed research. S.-H.H., B.-D.L., C.B.A., and F.K. contributed new analytical tools. Y.S., S.H., and N.-C.P. analyzed data and wrote the article.

REFERENCES

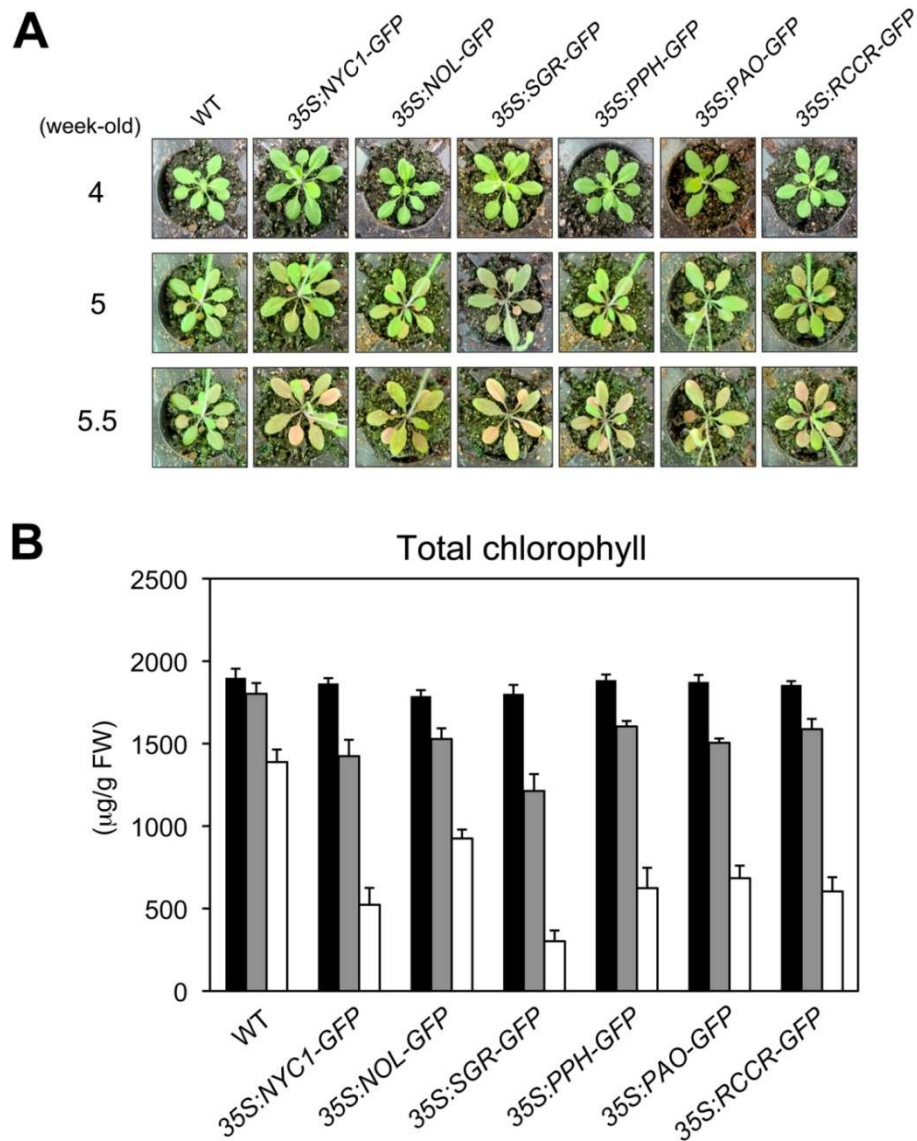
- Aubry, S., Mani, J., and Hörtensteiner, S. (2008). Stay-green protein, defective in Mendel's green cotyledon mutant, acts independent and upstream of pheophorbide *a* oxygenase in the chlorophyll catabolic pathway. *Plant Mol. Biol.* **67**: 243–256.
- Bracha-Drori, K., Shichrur, K., Katz, A., Oliva, M., Angelovici, R., Yalovsky, S., and Ohad, N. (2004). Detection of protein-protein interactions in plants using bimolecular fluorescence complementation. *Plant J.* **40**: 419–427.
- Earley, K.W., Haag, J.R., Pontes, O., Opper, K., Juehne, T., Song, K.M., and Pikaard, C.S. (2006). Gateway-compatible vectors for plant functional genomics and proteomics. *Plant J.* **45**: 616–629.
- Endler, A., Meyer, S., Schelbert, S., Schneider, T., Weschke, W., Peters, S.W., Keller, F., Baginsky, S., Martinoia, E., and Schmidt, U.G. (2006). Identification of a vacuolar sucrose transporter in barley and Arabidopsis mesophyll cells by a tonoplast proteomic approach. *Plant Physiol.* **141**: 196–207.
- Ginsburg, S., Schellenberg, M., and Matile, P. (1994). Cleavage of chlorophyll-porphyrin. Requirement for reduced ferredoxin and oxygen. *Plant Physiol.* **105**: 545–554.
- Guiboileau, A., Sormani, R., Meyer, C., and Masclaux-Daubresse, C. (2010). Senescence and death of plant organs: nutrient recycling and developmental regulation. *C. R. Biol.* **333**: 382–391.
- Horie, Y., Ito, H., Kusaba, M., Tanaka, R., and Tanaka, A. (2009). Participation of chlorophyll *b* reductase in the initial step of the degradation of light-harvesting chlorophyll *a/b*-protein complexes in *Arabidopsis*. *J. Biol. Chem.* **284**: 17449–17456.
- Hörtensteiner, S. (2004). The loss of green color during chlorophyll degradation—A prerequisite to prevent cell death? *Planta* **219**: 191–194.
- Hörtensteiner, S. (2006). Chlorophyll degradation during senescence. *Annu. Rev. Plant Biol.* **57**: 55–77.
- Hörtensteiner, S. (2009). Stay-green regulates chlorophyll and chlorophyll-binding protein degradation during senescence. *Trends Plant Sci.* **14**: 155–162.
- Hörtensteiner, S., and Feller, U. (2002). Nitrogen metabolism and remobilization during senescence. *J. Exp. Bot.* **53**: 927–937.
- Hörtensteiner, S., and Kräutler, B. (2011). Chlorophyll breakdown in higher plants. *Biochim. Biophys. Acta* **1807**: 977–988.
- Hörtensteiner, S., Vicentini, F., and Matile, P. (1995). Chlorophyll breakdown in senescent cotyledons of rape, *Brassica napus* L.: Enzymatic cleavage of pheophorbide *a* *in vitro*. *New Phytol.* **129**: 237–246.
- Jiang, H., Li, M., Liang, N., Yan, H., Wei, Y., Xu, X., Liu, J., Xu, Z., Chen, F., and Wu, G. (2007). Molecular cloning and function analysis of the *stay green* gene in rice. *Plant J.* **52**: 197–209.
- Jørgensen, K., Rasmussen, A.V., Morant, M., Nielsen, A.H., Bjarnholt, N., Zagrobely, M., Bak, S., and Møller, B.L. (2005). Metabolite formation and metabolic channeling in the biosynthesis of plant natural products. *Curr. Opin. Plant Biol.* **8**: 280–291.
- Joyard, J., Ferro, M., Masselon, C., Seigneurin-Berry, D., Salvi, D., Garin, J., and Rolland, N. (2009). Chloroplast proteomics and the compartmentation of plastidial isoprenoid biosynthetic pathways. *Mol. Plant* **2**: 1154–1180.
- Kräutler, B. (2008). Chlorophyll breakdown and chlorophyll catabolites in leaves and fruit. *Photochem. Photobiol. Sci.* **7**: 1114–1120.
- Kräutler, B., Jaun, B., Bortlik, K.-H., Schellenberg, M., and Matile, P. (1991). On the enigma of chlorophyll degradation: the constitution of a secoporphinoid catabolite. *Angew. Chem. Int. Ed. Engl.* **30**: 1315–1318.
- Kreuz, K., Tommasini, R., and Martinoia, E. (1996). Old enzymes for a new job. Herbicide detoxification in plants. *Plant Physiol.* **111**: 349–353.
- Kusaba, M., Ito, H., Morita, R., Iida, S., Sato, Y., Fujimoto, M., Kawasaki, S., Tanaka, R., Hirochika, H., Nishimura, M., and Tanaka, A. (2007). Rice NON-YELLOW COLORING1 is involved in light-harvesting complex II and grana degradation during leaf senescence. *Plant Cell* **19**: 1362–1375.
- Lim, P.O., Kim, H.J., and Nam, H.G. (2007). Leaf senescence. *Annu. Rev. Plant Biol.* **58**: 115–136.
- Mach, J.M., Castillo, A.R., Hoogstraten, R., and Greenberg, J.T. (2001). The *Arabidopsis*-accelerated cell death gene *ACD2* encodes

- red chlorophyll catabolite reductase and suppresses the spread of disease symptoms. *Proc. Natl. Acad. Sci. USA* **98**: 771–776.
- Matile, P., Hörtensteiner, S., and Thomas, H.** (1999). Chlorophyll degradation. *Annu. Rev. Plant Physiol. Plant Mol. Biol.* **50**: 67–95.
- Matile, P., and Schellenberg, M.** (1996). The cleavage of pheophorbide *a* is located in the envelope of barley gerontoplasts. *Plant Physiol. Biochem.* **34**: 55–59.
- Matile, P., Schellenberg, M., and Peisker, C.** (1992). Production and release of a chlorophyll catabolite in isolated senescent chloroplasts. *Planta* **187**: 230–235.
- Meguro, M., Ito, H., Takabayashi, A., Tanaka, R., and Tanaka, A.** (2011). Identification of the 7-hydroxymethyl chlorophyll *a* reductase of the chlorophyll cycle in *Arabidopsis*. *Plant Cell* **23**: 3442–3453.
- Meyer, A., Eskandari, S., Grallath, S., and Rentsch, D.** (2006). AtGAT1, a high affinity transporter for gamma-aminobutyric acid in *Arabidopsis thaliana*. *J. Biol. Chem.* **281**: 7197–7204.
- Mochizuki, N., Tanaka, R., Grimm, B., Masuda, T., Moulin, M., Smith, A.G., Tanaka, A., and Terry, M.J.** (2010). The cell biology of tetrapyrroles: a life and death struggle. *Trends Plant Sci.* **15**: 488–498.
- Morita, R., Sato, Y., Masuda, Y., Nishimura, M., and Kusaba, M.** (2009). Defect in non-yellow coloring 3, an alpha/beta hydrolase-fold family protein, causes a stay-green phenotype during leaf senescence in rice. *Plant J.* **59**: 940–952.
- Oberhuber, M., Berghold, J., Breuker, K., Hörtensteiner, S., and Kräutler, B.** (2003). Breakdown of chlorophyll: a nonenzymatic reaction accounts for the formation of the colorless “nonfluorescent” chlorophyll catabolites. *Proc. Natl. Acad. Sci. USA* **100**: 6910–6915.
- Park, S.-Y., et al.** (2007). The senescence-induced staygreen protein regulates chlorophyll degradation. *Plant Cell* **19**: 1649–1664.
- Porra, R.J., Thompson, W.A., and Kriedemann, P.E.** (1989). Determination of accurate extinction coefficients and simultaneous equations for assaying chlorophyll *a* and chlorophyll *b* extracted with 4 different solvents: Verification of the concentration of chlorophyll standards by atomic absorption spectroscopy. *Biochim. Biophys. Acta* **975**: 384–394.
- Pružinská, A., Anders, I., Aubry, S., Schenk, N., Tapernoux-Lüthi, E., Müller, T., Kräutler, B., and Hörtensteiner, S.** (2007). In vivo participation of red chlorophyll catabolite reductase in chlorophyll breakdown. *Plant Cell* **19**: 369–387.
- Pružinská, A., Tanner, G., Anders, I., Roca, M., and Hörtensteiner, S.** (2003). Chlorophyll breakdown: Pheophorbide *a* oxygenase is a Rieske-type iron-sulfur protein, encoded by the *accelerated cell death 1* gene. *Proc. Natl. Acad. Sci. USA* **100**: 15259–15264.
- Pružinská, A., Tanner, G., Aubry, S., Anders, I., Moser, S., Müller, T., Ongania, K.-H., Kräutler, B., Youn, J.-Y., Liljegren, S.J., and Hörtensteiner, S.** (2005). Chlorophyll breakdown in senescent *Arabidopsis* leaves. Characterization of chlorophyll catabolites and of chlorophyll catabolic enzymes involved in the degreening reaction. *Plant Physiol.* **139**: 52–63.
- Ren, G., An, K., Liao, Y., Zhou, X., Cao, Y., Zhao, H., Ge, X., and Kuai, B.** (2007). Identification of a novel chloroplast protein AtNYE1 regulating chlorophyll degradation during leaf senescence in *Arabidopsis*. *Plant Physiol.* **144**: 1429–1441.
- Ren, G.D., Zhou, Q., Wu, S.X., Zhang, Y.F., Zhang, L.G., Huang, J.R., Sun, Z.F., and Kuai, B.K.** (2010). Reverse genetic identification of CRN1 and its distinctive role in chlorophyll degradation in *Arabidopsis*. *J. Integr. Plant Biol.* **52**: 496–504.
- Rodoni, S., Mühlecker, W., Anderl, M., Kräutler, B., Moser, D., Thomas, H., Matile, P., and Hörtensteiner, S.** (1997). Chlorophyll breakdown in senescent chloroplasts. Cleavage of pheophorbide *a* in two enzymic steps. *Plant Physiol.* **115**: 669–676.
- Sakuraba, Y., Yokono, M., Akimoto, S., Tanaka, R., and Tanaka, A.** (2010). Deregulated chlorophyll *b* synthesis reduces the energy transfer rate between photosynthetic pigments and induces photodamage in *Arabidopsis thaliana*. *Plant Cell Physiol.* **51**: 1055–1065.
- Sato, Y., Morita, R., Katsuma, S., Nishimura, M., Tanaka, A., and Kusaba, M.** (2009). Two short-chain dehydrogenase/reductases, NON-YELLOW COLORING 1 and NYC1-LIKE, are required for chlorophyll *b* and light-harvesting complex II degradation during senescence in rice. *Plant J.* **57**: 120–131.
- Sato, Y., Morita, R., Nishimura, M., Yamaguchi, H., and Kusaba, M.** (2007). Mendel’s green cotyledon gene encodes a positive regulator of the chlorophyll-degrading pathway. *Proc. Natl. Acad. Sci. USA* **104**: 14169–14174.
- Scheibe, R., Wedel, N., Vetter, S., Emmerlich, V., and Saueremann, S.M.** (2002). Co-existence of two regulatory NADP-glyceraldehyde 3-P dehydrogenase complexes in higher plant chloroplasts. *Eur. J. Biochem.* **269**: 5617–5624.
- Schelbert, S., Aubry, S., Burla, B., Agne, B., Kessler, F., Krupinska, K., and Hörtensteiner, S.** (2009). Pheophytin pheophorbide hydrolase (pheophytinase) is involved in chlorophyll breakdown during leaf senescence in *Arabidopsis*. *Plant Cell* **21**: 767–785.
- Schenk, N., Schelbert, S., Kanwischer, M., Goldschmidt, E.E., Dörmann, P., and Hörtensteiner, S.** (2007). The chlorophyllases AtCLH1 and AtCLH2 are not essential for senescence-related chlorophyll breakdown in *Arabidopsis thaliana*. *FEBS Lett.* **581**: 5517–5525.
- Shlyk, A.A.** (1971). Biosynthesis of chlorophyll *b*. *Annu. Rev. Plant Physiol.* **22**: 169–184.
- Takamiya, K.I., Tsuchiya, T., and Ohta, H.** (2000). Degradation pathway(s) of chlorophyll: What has gene cloning revealed? *Trends Plant Sci.* **5**: 426–431.
- Tanaka, R., Hirashima, M., Satoh, S., and Tanaka, A.** (2003). The *Arabidopsis*-accelerated cell death gene ACD1 is involved in oxygenation of pheophorbide *a*: Inhibition of the pheophorbide *a* oxygenase activity does not lead to the “stay-green” phenotype in *Arabidopsis*. *Plant Cell Physiol.* **44**: 1266–1274.
- Tanaka, R., and Tanaka, A.** (2007). Tetrapyrrole biosynthesis in higher plants. *Annu. Rev. Plant Biol.* **58**: 321–346.
- Thomas, H., and Howarth, C.J.** (2000). Five ways to stay green. *J. Exp. Bot.* **51**(Spec No): 329–337.
- Thomas, H., Ougham, H.J., Wagstaff, C., and Stead, A.D.** (2003). Defining senescence and death. *J. Exp. Bot.* **54**: 1127–1132.
- Vidi, P.A., Kanwischer, M., Baginsky, S., Austin, J.R., Csucs, G., Dörmann, P., Kessler, F., and Bréhélin, C.** (2006). Tocopherol cyclase (VTE1) localization and vitamin E accumulation in chloroplast plastoglobule lipoprotein particles. *J. Biol. Chem.* **281**: 11225–11234.
- Zavaleta-Mancera, H.A., Franklin, K.A., Ougham, H.J., Thomas, H., and Scott, I.M.** (1999a). Regreening of senescent *Nicotiana* leaves I. Reappearance of NADPH-protochlorophyllide oxidoreductase and light-harvesting chlorophyll *a/b*-binding protein. *J. Exp. Bot.* **50**: 1677–1682.
- Zavaleta-Mancera, H.A., Thomas, B.J., Thomas, H., and Scott, I.M.** (1999b). Regreening of senescent *Nicotiana* leaves II. Redifferentiation of plastids. *J. Exp. Bot.* **50**: 1683–1689.
- Zhang, X.R., Henriques, R., Lin, S.S., Niu, Q.W., and Chua, N.H.** (2006). *Agrobacterium*-mediated transformation of *Arabidopsis thaliana* using the floral dip method. *Nat. Protoc.* **1**: 641–646.



Supplemental Figure 1. Subcellular Localization of SGR-GFP and CCE-GFP Fusion Proteins in Transgenic Plants.

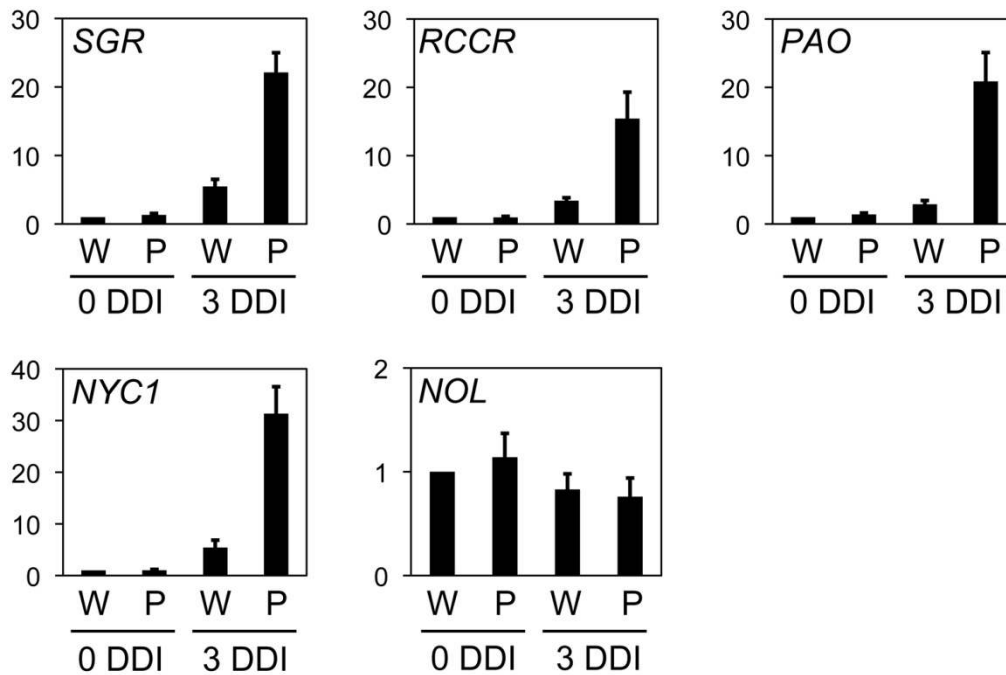
Green rosette leaves of 3-week-old transgenic plants were homogenized with protein extraction buffer, and membrane-enriched and soluble fractions were subjected to SDS-PAGE. GFP-fusion proteins were detected by immunoblotting with α -GFP using an ECL detection system (15 sec exposure). Only when the immunoblots were exposed for much longer (1 min exposure), fine and weak bands of GFP-tagged proteins were seen in soluble fractions, indicating that SGR and CCEs largely localize in the membrane fractions. CBB-stained membrane-enriched and soluble fractions are shown as loading controls.



Supplemental Figure 2. Natural senescence of *Arabidopsis* SGR-GFP and CCE-GFP overexpressors.

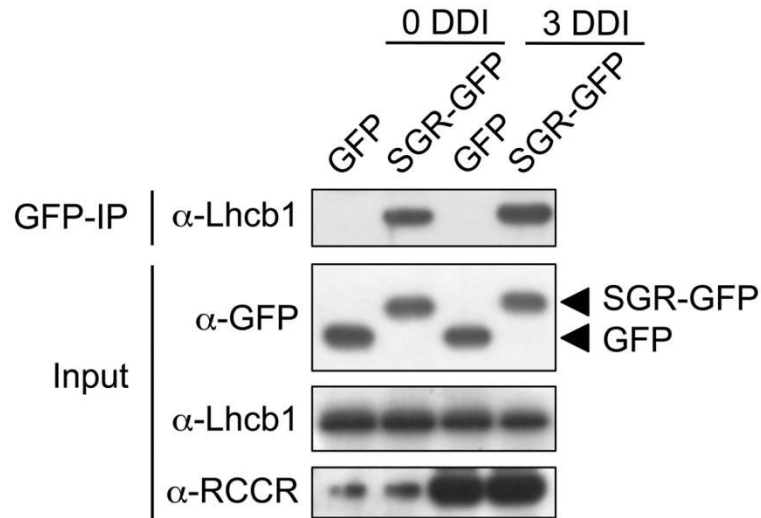
(A) Visible phenotypes of WT and SGR/CCE-GFP overexpressor lines during natural senescence. Photographs were taken at 4, 5, and 5.5 weeks after germination under long day condition.

(B) Degradation of Chl in WT and SGR/CCE-GFP overexpressor lines during natural senescence. Black, gray, and white bars indicate Chl levels of entire rosette leaves of 4-, 5-, and 5.5-week-old plants, respectively. Mean and SD values were obtained from at least five replicates.



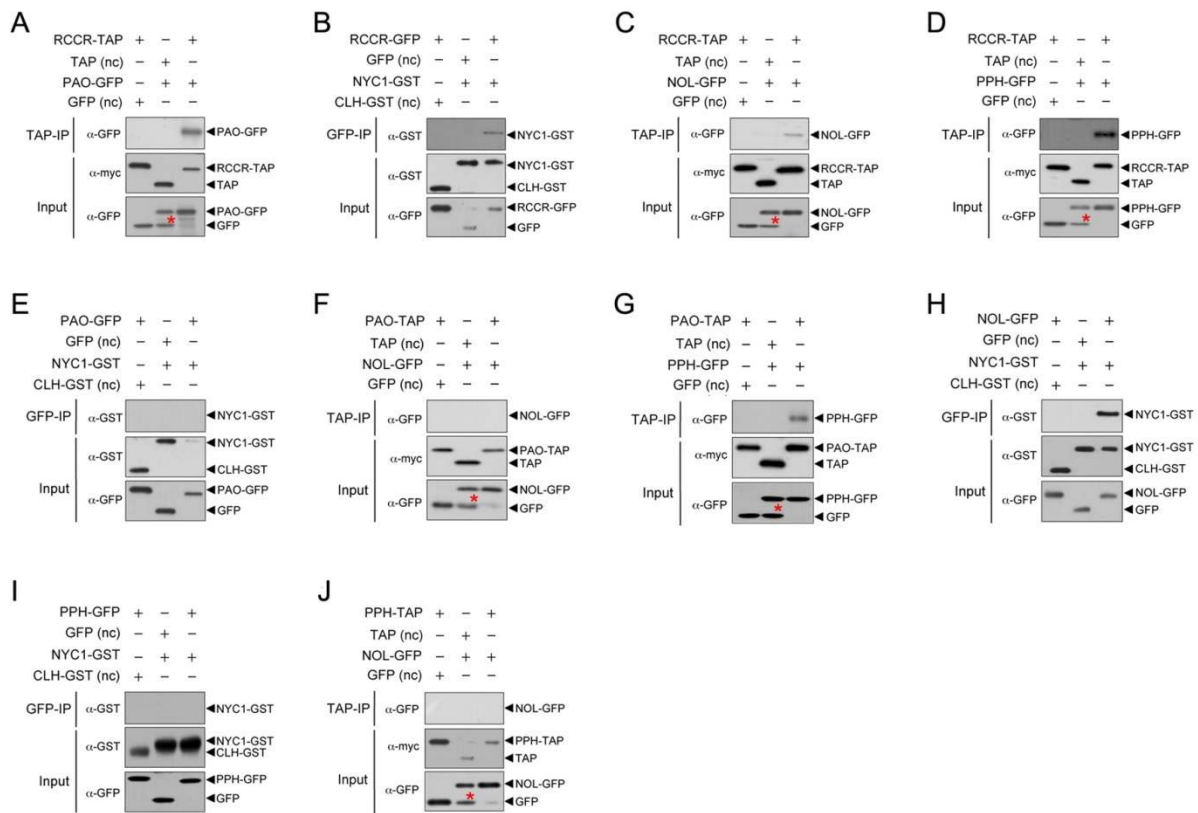
Supplemental Figure 3. Expression Analysis of Genes Encoding SGR and four CCEs in WT (W) and *35S:PPH-GFP* (P) Leaves by qRT-PCR.

The mRNA levels of *SGR* and four CCE genes (*RCCR*, *PAO*, *NYC1*, and *NOL*) were measured before (0 DDI) and after 3 d of dark-induced senescence (3 DDI). The relative mRNA levels were normalized to the transcript levels of *GAPDH* (glyceraldehyde phosphate dehydrogenase; At1g16300). Mean and SD values were obtained from at least nine replicates.

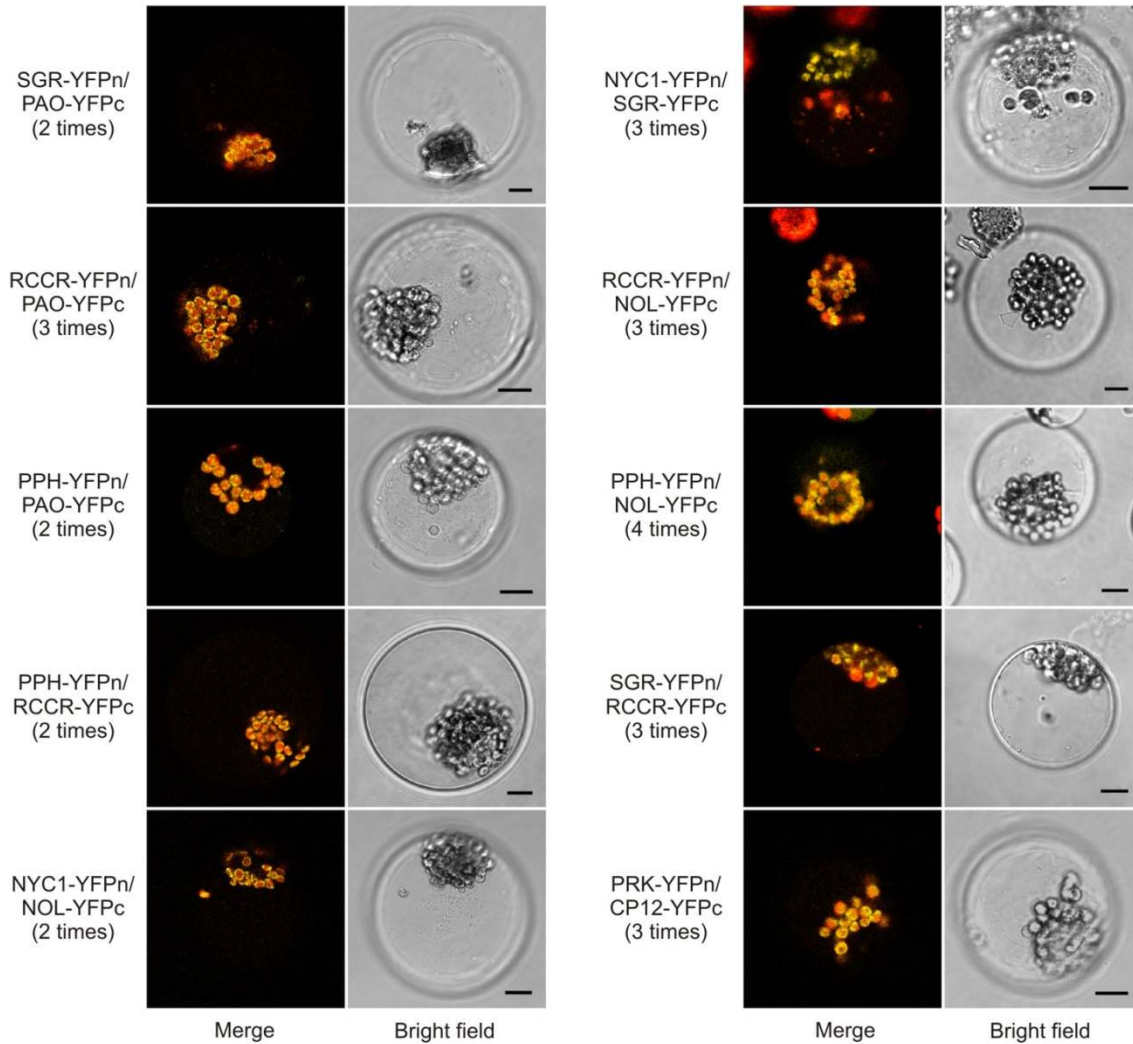


Supplemental Figure 4. *Arabidopsis* SGR Interacts with LHCII in Senescent as well as Non-Senescent Chloroplasts.

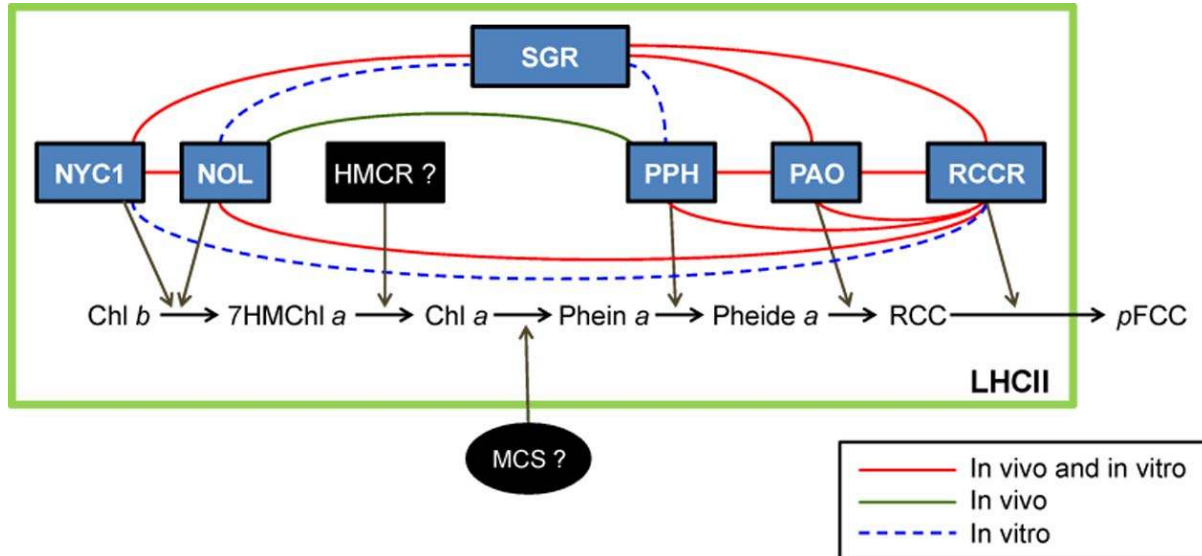
Transgenic *Arabidopsis* lines expressing GFP-tagged SGR constitutively (*35S:SGR-GFP*) were used before (0 DDI) and after 3 d of dark-induced senescence (3 DDI) for pull-down experiments with α -GFP-conjugated beads (GFP-IP). Interaction with LHCII was examined with α -Lhcb1. The *35S:GFP* plants were used as negative control. The input levels of tagged proteins and Lhcb1 are shown.



Supplemental Figure 5. Interactions among CCEs by In Vitro Pull-Down Assays. Equal fresh weight of rosette leaves of two 3-week-old *Arabidopsis* plants expressing tagged CCEs were co-homogenized. Membrane-enriched fractions were used for pull-down assays with α -GFP- (GFP-IP) or IgG-conjugated beads (TAP-IP). Ten combinations, i.e. RCCR-PAO (**A**), RCCR-NYC1 (**B**), RCCR-NOL (**C**), RCCR-PPH (**D**), PAO-NYC1 (**E**), PAO-NOL (**F**), PAO-PPH (**G**), NOL-NYC1 (**H**), PPH-NYC1 (**I**), and PPH-NOL (**J**), were examined. As the results in yeast two-hybrid assays (Figure 4), the interactions of PAO-NYC1 (**E**), PAO-NOL (**F**), PPH-NYC1 (**I**), and PPH-NOL (**J**) were negative in this assay. *35S::GFP*, *35S::TAP* and *35S::CLH-GST* plants were used as negative controls (nc). Input levels of tagged proteins detected with respective antibodies are shown. Asterisks (red) mark TAP proteins (negative control) as detected by α -GFP.



Supplemental Figure 6. In Vivo Interactions among SGR and CCEs Analyzed by BiFC. For BiFC assays, construct pairs expressing fusions between SGR or CCEs, and the N- or C-terminal half of YFP (YFPn or YFPc, respectively) were co-expressed in *Arabidopsis* mesophyll protoplasts isolated from 4 DDI-senescing rosette leaves. Confocal microscopic analysis was performed after 24 h. Note that only positive interactions, i.e. SGR-PAO, RCCR-PAO, PPH-PAO, PPH-RCCR, NYC1-NOL, NYC1-SGR, RCCR-NOL, PPH-NOL and SGR-RCCR, are shown. The positive control between PRK and CP12 is depicted as well. Numbers in brackets indicate the number of independent transformation experiment performed with each combination. Combinations that resulted in negative BiFC interaction, i.e. SGR-PPH, SGR-NOL, PAO-NYC1 and PAO-NOL, are not shown. Each of these was also tested independently at least twice. Two combinations, RCCR-NYC1 and PPH-NYC1, were not tested. Note that besides bright field images, only merged pictures of YFP- (yellow) and Chl autofluorescence (red) are shown. Bars = 10 μ m.



Supplemental Figure 7. Possible Metabolic Channeling of Chl Catabolic Intermediates by Interaction of SGR, CCEs and LHCII at the Thylakoid Membrane.

Taking together the interaction results of this study (yeast two-hybrid, in vitro and in vivo pull-down, and BiFC assays), we propose that Chl detoxification during leaf senescence occurs by metabolic channeling of Chl catabolites through direct and indirect interaction of SGR and CCEs in LHCII, thereby forming a SGR-CCE-LHCII complex. HMCR, which converts 7-hydroxymethyl Chl *a* (7HMChl *a*) to Chl *a*, has been recently discovered at the molecular level (Meguro et al., 2011), and it remains to be determined whether HMCR is an additional component of the SGR-CCE-LHCII complex. Colored lines indicate respectively, in vitro (yeast two-hybrid and in vitro pull-down assays) and/or in vivo (BiFC) confirmation of interaction as determined in this work.

Supplemental Table 1. *Arabidopsis* Transformants Expressing Tagged Versions of SGR and CCEs Used in This Study.

Gene	Accession	Transformants	Predicted fusion protein size (kD)*
<i>SGR</i>	At4g22920	<i>35S:SGR-GFP</i>	51.7
		<i>35S:SGR-GST</i>	50.6
<i>RCCR</i>	At4g37000	<i>35S:RCCR-GFP</i>	58.9
		<i>35S:RCCR-TAP</i>	56.9
<i>NYC1</i>	At4g13250	<i>35S:NYC1-GFP</i>	77.0
		<i>35S:NYC1-GST</i>	75.9
<i>NOL</i>	At5g04900	<i>35S:NOL-GFP</i>	58.4
<i>PPH</i>	At5g13800	<i>35S:PPH-GFP</i>	76.4
		<i>35S:PPH-TAP (N)**</i>	74.4
<i>PAO</i>	At3g44880	<i>35S:PAO-GFP</i>	82.3
		<i>35S:PAO-TAP</i>	80.3

* Predicted size of each protein was calculated without the chloroplast targeting signal. Lengths of chloroplast targeting signals were determined using TargetP (www.cbs.dtu.dk/services/TargetP).

** (N) indicate fusion proteins obtained from transient overexpression in *Nicotiana benthamiana*.

Supplemental Table 2. Primers Used in This Study.

Gene	Forward primer (5'→3')	Reverse primer (5'→3')
<i>A. Transgenic plants</i>		
<i>GFP- and TAP-tag constructs</i>		
<i>SGR</i>	ATGTGTAGTTTGTCTGGCGATTATG	GAGTTTCTCCGGATTTGGA
<i>RCCR</i>	ATGGCGATGATATTTTGCAACACTC	GAGAACACCGAAAGCTTCTTTAA
<i>PPH</i>	ATGGAGATAATCTCACTGAACG	TGCAGACTTCCCTCCAAA
<i>PAO</i>	ATGTCAGTAGTTTTACTCTCTTCT	CTCGATTTT CAGAATGTACATA
<i>NYC1</i>	ATGACTACTTTAACGAAGATTCA	TGTGCCTGGAAAAGAGCTA
<i>NOL</i>	ATGGCTACTTGGAGTGGTTTC	CTCTTCAGTAACATACCTGT
<i>GST-tag constructs</i>		
<i>SGR</i>	TCTAGATGTGTAGTTTGTCTGGCGAT	GGATCCGAGTTTCTCCGGATTTGGA
<i>NYC1</i>	TCTAGATGACTACTTTAACGAAG	GGATCCTGTGCCTGGAAAAGAGC
<i>B. qRT-PCR</i>		
<i>SGR</i>	GGTGGCCATTTCTTTTAGA	TCAACAAGTTCCCATCTCCA
<i>RCCR</i>	CGCCGAAAATTTATGGAGTT	AGGGAAGGAGTTGTGATTGG
<i>NYC1</i>	TTCTCAGTGGTTCGAGCATT	AGGTAATTGACGGCTTTTCC
<i>NOL</i>	TGCAGATGCAAGATGTCAAA	TGGTGTAGGCTTTGATTCCA
<i>PAO</i>	CTCTGGTTTGATCGGAATGAT	GAAGCTCGTGCTGTAAATCC
<i>GAPDH</i>	TTGGTGACAACAGGTCAAGCA	AAACTTGTGCTCAATGCAATC
<i>C. BiFC assay</i>		
<i>PPH</i>	CGTTCATGAAGATAATCTCACTGAACGTTG	TAAAGCGGCCGCGCAGACTTCCCTCCAAACAC
<i>PAO</i>	CGTTCATGACAGTAGTTTTACTCTCTTCTAC	TAAAGCGGCCGCTCGATTT CAGAATGTACAT
<i>SGR</i>	CGTTCATGAGTAGTTTGTCTGGCGATTATG	TAAAGCGGCCGCGAGTTTCTCCGGATTTGGA
<i>RCCR</i>	CGTTCATGACGATGATATTTTGCAACACTC	TAAAGCGGCCGCGAGAACACCGAAAGCTTCTTT
<i>NYC1</i>	CGTTCATGACTACTTTAACGAAGATTCAAG	TAAAGCGGCCGCGTGCCTGGAAAAGAGCTAGG
<i>NOL</i>	CGTTCATGACTACTTGGAGTGGTTTCAACG	TAAAGCGGCCGCTCTTCAGTAACATACCTGTT
<i>D. PAO-GFP construct</i>		
<i>PAO</i>	GAAGATCTATGTCAGTAGTTTTACTCTCTTC	GCTCTAGACTCGATTT CAGAATGTACATAATC